A Generalized Natural Hazard Risk Modelling Framework for Infrastructure Failure Cascades

Evelyn Mühlhofer[a,b*], Elco E. Koks[c], Chahan M. Kropf[a,b], Giovanni Sansavini[d], David N. Bresch[a,b]

[a] *Institute for Environmental Decisions, ETH Zurich, Zurich, 8092, Switzerland*
[b] *Federal Office of Meteorology and Climatology MeteoSwiss, Zurich-Airport, 8058, Switzerland*
[c] *Institute for Environmental Studies, VU Amsterdam, Amsterdam, The Netherlands*
[d] *Institute of Energy and Process Engineering, ETH Zurich, Zurich, 8092, Switzerland*

[*]corresponding author (evelyn.muelhofer@usys.ethz.ch)

non-peer reviewed preprint submitted to EarthArXiv
submitted for peer review to Reliability Engineering & Systems Safety

Abstract

Critical infrastructures are more exposed than ever to natural hazards in a chaning climate. To understand and manage risk, failure cascades across large, real-world infrastructure networks, caused by real-world hazards, and their impact on people, must be captured. Bridging established methods in both infrastructure and risk modelling communities, we develop an open-source modelling framework which integrates a network-based interdependent infrastructure system model into the globally consistent and spatially explicit natural hazard risk assessment platform CLIMADA. The model captures infrastructure damages, triggers failure cascades and estimates resulting basic service disruptions for the dependent population. It flexibly operates on large areas with publicly available hazard, exposure and vulnerability information, for any infrastructure networks, hazards and geographies of interest. In a validated case study for 2018's Hurricane Michael across three US states, the model reproduced important failure dynamics among six infrastructure networks, and provided a novel spatial map of where people were likely to experience disruptions in access to healthcare, loss of power and other vital services. Our generalized approach allows for a view on infrastructure risks and their social impacts also in areas where detailed information and risk assessments are traditionally scarce, informing humanitarian activities through hotspot analyses and policy frameworks alike.

Highlights

- Develops an interoperable impact framework, from hazards to CI failures and basic service disruptions
- Couples an infrastructure network model to a natural hazard risk assessment platform
- Implements a model design for real-world, large interdependent CI systems, applicable across the globe
- Demonstrates and validates the model for a hurricane event in 3 US states and 6 CI systems

Keywords
Risk assessment, natural hazards, critical infrastructures, failure cascades, basic services, system-of-systems

1. Introduction

When natural hazards disrupt critical infrastructures (CIs), their failure can be detrimental to public health, safety, security, well-being and economic activities [1]. Whether due to an earthquake in Japan, a flooding across Western Europe or a hurricane hitting the US, lifeline disruptions are ubiquitous: loss of power and telecommunication services may compound with a dysfunctional transport system and damaged hospitals, preventing emergency responders to intervene timely, rendering villages inaccessible for days, cutting off evacuation routes, or leaving school children without access to education for up to weeks [2]–[5].

As infrastructure investments are at an all-time high [6], CI systems around the globe are more than ever exposed to natural hazards, a trend which is further exacerbated in a changing climate [7]. This poses a threat to air, road and rail transportation alike [8], [9], puts power generation at risk [10] and causes losses of billions of US dollars annually in several CI sectors [9], [10].

Since societal impacts of CI failures tend to reach far beyond the technical sphere, managing resilient infrastructure has become a prime area of concern for policy makers: CIs "directly or indirectly influence the attainment of all of the SDGs" [6] and may accrue up to 88% of all climate adaptation costs until 2050 [11]. Reducing disaster damage from CIs and basic service disruptions forms part of the agendas of the Sendai Framework for Disaster Risk Reduction, the European Commission's Programme for Critical Infrastructure Protection (EPCIP) and the 26th UN Climate Change Conference (COP26) alike. Though different in scope and nature, three key challenges of CIs in a socio-technical context are recurrent: Knowledge on the extent to which CIs are exposed to natural hazards is insufficient, especially in the Global South (cf. §25 e and f in [12]); interdependences between different CIs are often poorly understood, and cascading effects from CI failures are difficult to analyse and hence manage systematically [13], [14] ; the experienced hardship from CI failures depends on the degree and duration to which basic services are disrupted [15], yet the link between infrastructure damages, resulting service outages and affected population is not straightforward.

Capturing the response of interdependent CI systems to natural disasters, and studying the impacts of their failures onto the population, is an endeavour residing at the intersection of natural hazard (NH) risk modelling, infrastructure modelling and social vulnerability research. Traditionally, those problems have been approached with community-specific research questions and methods:

NH risks emerge through the interplay of weather and climate-related hazards, the exposure of (infrastructure) assets, goods and people to those hazards and their specific vulnerabilities (IPCC 2014). Event-based impact modelling therefore commonly relies on those three components to calculate expectable asset damages to CIs as a proxy of direct risk [16]. Efforts to capture risk levels for CIs globally are often challenged by data availability (cf. [17]), yet have been undertaken for a few hazards and CI sectors such as road, rail, airports and power generation [8], [9], [18]. Despite acknowledging the importance to embrace a systems-thinking approach for resilience [19], [20], NH risk modelers' predominant focus on 'asset scale risk' [20] often runs short of capturing CI interdependencies and

'network scale risks'. As such, the community's risk assessment methods are not yet tailored to the specificities of CIs.

In infrastructure research, CI interdependences and failure cascades have received much attention since the seminal work of Rinaldi et al. [14] and approaches to model CI 'system-of-systems' [21] have converged to several state-of-the art methods [22]. Especially in studies employing network (flow) approaches (cf. [23]), NH-induced failure triggers have motivated research on cascades [24]–[29]. Yet, most research in this domain shares some of the following tendencies: Investigated systems are mostly small-scale, representative of mid-sized towns or single community districts and illustrate dynamics for a sub-system of two infrastructure types [28], [30]–[33] (see [25], [27], [34] for counter-examples) where power, transport and telecommunication systems are investigated much more often than social facilities such as schools or hospitals. CI data is frequently based on artificial, well-defined test-beds [24], [33], [35], [36], or tailored to the (sometimes proprietary) data at hand, which is overwhelmingly based in the US, Europe and Oceania [25], [32], [37], [38]. Failure scenarios often focus on random or component-wise removals [34], [39], [40], or feature stylized shapes in lack of realistic hazard footprints [25], [35]. Study scopes and trigger mechanisms in existing CI research are hence not necessarily tailored to capture the magnitude and spatial extents of real-world NH events and CI systems.

Lastly, the technical discourse on CI failures, where impact metrics focus predominantly on functional performance benchmarks, does not link adequately to the domain of social vulnerabilities [41]. Apart from empirical case-studies using print media accounts [42], only few modelling studies have explored consequences of CI failures for (socio-economically different groups of) people [43], [44].

Despite advances in tackling this common problem space, silos persist which have inspired several frameworks on systemic CI risks at a national analysis level [20], [21]. Following this logic, our aim is to provide a flexible hazard-to-human impact model which estimates spatial patterns of people experiencing basic service disruptions caused by natural hazard-induced CI failure cascades. The model is built on top of open-source data, and capable to assess the impacts for large areas, and different CI systems and hazards of interest. In line with Zio [1], who stresses the need to integrate different modelling perspectives to capture complexities of CI system failures, we showcase how synergies can be yielded by combining established methods and platforms used by CI researchers and NH risk modellers. The focus of this work is on scale, transferability and interoperability. Impact estimates produced with this approach are hence thought to inform rapid hotspot assessments during emergency responses, or as a comparable, human-centric measure of risk for policy purposes in international frameworks.

Chapter 2 develops the methodological framework required to link a CI systems model to a NH model, under the conditions of working with large systems, limited process knowledge and data availability, and ease of transferability. The framework is implemented as an end-to-end modelling chain, embedded in the open-source risk modelling platform CLIMADA [45]. Chapter 3 demonstrates how the model can provide information services in the aftermath of disaster within a case study of a historic tropical cyclone hitting

the Florida Panhandle. Detailed sensitivity analyses and results validation are included. Chapter 4 discusses the merits and trade-offs of this approach, and examines its adequacy and extension possibilities for use in risk assessments, adaptation planning and policy making.

2. Methods

The framework in Figure 2.1 illustrates the major conceptual stages developed to calculate basic service disruptions from natural hazard-induced infrastructure failure cascades.

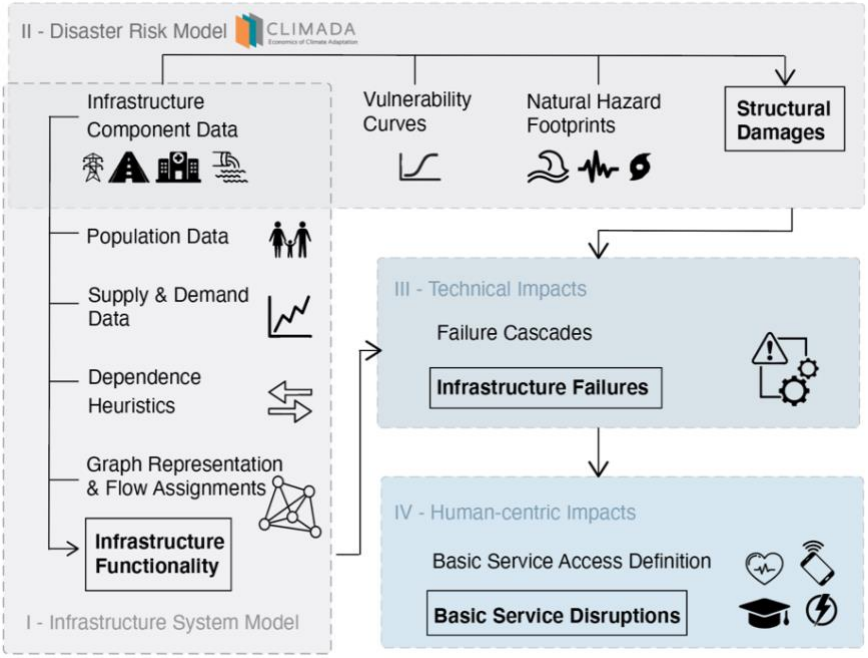

Figure 2.1 Generic framework to estimate the population experiencing basic service disruptions from natural hazard-induced infrastructure failure cascades. The four stages encompass infrastructure system modelling (I), disaster risk modelling (II), and two results layers - infrastructure component failures from failure cascades (III) and basic service disruptions to the population (IV).

Stage I develops an infrastructure system model to represent the functional state of interdependent critical infrastructures and their dependent population. Inspired by established network (flow) approaches [34] and using dependency heuristics when needed, geo-coded information on infrastructure components and on population, supply and demand data are combined in a graph. In stage II structural damages to infrastructure components are computed from spatially explicit hazard footprints and tailored vulnerability curves, using the risk modelling platform CLIMADA. Stage III feeds results from structural damage calculations back into the infrastructure system model, which triggers failures cascades along infrastructure dependencies. This yields results on a technical system impact level. In stage IV, technical impacts of CI failures are translated to human-centric impacts. Resulting disruptions to basic service access are computed for all services provided by the CI systems under study, for the dependent population. The following sections describe the formal implementation of the framework and its embedding within CLIMADA; for a list of abbreviations used throughout the text and a condensed summary, see annex A.

2.1. Stage I: Infrastructure System Model

2.1.1. Infrastructure Component and Population Data

Geographic data on infrastructure networks is collected at a component (i.e. asset) level for the area of interest, such as the location of schools, roads or electrical power plants in a country, state or greater metropolitan area from open-source data providers such as OpenStreetMap, unless already at hand. A first step of complexity reduction and standardization consists in limiting the structural components per CI system to a few main building blocks or components. For instance, the road network can be reduced to intersections (nodes) and streets (edges), ignoring bridges and tunnels (c.f. Table B.1 for a possible components selection for six main types of CI networks at various resolutions). The use of the term *CI network* will henceforth refer to these physical, simplified, real-world infrastructures. Population data can be obtained at high resolution from globally available sources such as the WorldPop project [46].

As a stylized example throughout the remainder of the model description, we consider the communication (c), electric power (e) and health (h) networks represented through their most crucial components (cell towers, power plants, transmission lines, poles, and hospitals), and population grid cells (p) representing end-users, as illustrated in Figure 2.2, panel A.1.

2.1.2. Graph Representations

Infrastructure components are hence transformed into directed graphs consisting in nodes and edges. In our example, the power network's plant and poles are represented by nodes and power lines as edges, while the graphs for communication and healthcare networks are made up of nodes only (see Figure 2.2, panel A.1 (centre)). These formal representations will henceforth be referred to as *CI graph* G^j , where *j* is the system type (e.g. G^e for the electric power CI graph). In addition, geographical location *L*, initial functional state F^0 and the infrastructure-specific damage threshold D^j are set as attributes for all elements (nodes and edges) in each CI graph. F^0 is set to 1 for all elements. D^j indicates the structural damage fraction beyond which a component will lose its functionality and is a simplifiying concept to derive functional states from damages. Thresholds are set arbitrarily in this example for purely illustrative purposes. The population network similarly is represented by a node-containing graph with people counts and geographical location as node attributes.

2.1.3. Developing Dependency Heuristics

To identify functional dependencies which exist in between CI networks, and between CI networks and their end-users (population), a standardized rule set was developed. From an extensive review on CI interdependence models, a list of 120 distinct dependencies between components of 11 different CI networks was collected (see Supplementary Materials) and consolidated within six generic rules, referred to as '*dependency heuristics*', and described in Table 2.1. Those rules can be refined and quantified according to the case study at hand, yet serve as a first starting point to infer dependencies between large CI networks.

Table 2.1 Synthesis of heuristics to infer dependencies between CI components of different systems and their users.

Rule #	Description
1	Most CI networks depend on electric power supply, telecommunications access and (cooling) water supply.
2	People-hosting facilities (e.g. hospitals, schools, power plants) depend on road access.

3	Dependencies can be categorized into either having redundant character, where several sources can provide necessary support (e.g. telecommunication access from any reachable cell), or being unique, where support is provided from a unique source (e.g. power from the single closest power line).
4	Dependencies are distance-constrained (e.g. a cell tower located 500 km away will not provide relevant service, neither will a hospital which is 1500 km across the country).
5	Dependencies may entail a continuous, physical flow between source and target (e.g. water, electricity), yet can be approximated through a binary, logical connection.
6	Population (end-users) depends on CIs for services, but not vice-versa.

A quantitative implementation of the developed dependency heuristics on the level of the CI graphs is obtained via a dependency-search algorithm based on the provision of source-target network pairs and four conditions: distance threshold, redundancy, road access and flow. The conditions are described in more detail in Table 2.2. First, for each pair of CI graphs (G^j,G^k), the algorithm places directed edges e^{jk} (dependencies) from sources nodes in G^j to target nodes in G^k when the conditions are fulfilled for the corresponding pair of network nodes. The dependency-search algorithm equally allows assignment of end-users to CI networks in the absence of more detailed, yet often proprietary utility providers' customer data; the population graph is then the target of infrastructure - end user pairs (G^j,G^p) for any relevant infrastructure type *j* - see example in Table 2.2, column 'Dep. C'. The algorithm hence results in the creation of one *interdependent CI graph G* from all CI graphs and the population graph. This is illustrated in Figure 2.2, panel A.1 (right).

Table 2.2 Required variables to characterize dependency establishment conditions between CI graphs. 'Source' and 'target' are CI network components of different systems, previously identified from the heuristics in Table 2.1. Three exemplary illustrations of dependencies are given; reading example Dep. A - Hospital depends on mobile communication access, which is assumed to be provided by any (redundancy=True) cell tower within a specified radius (30 km), without the need for a road to exist between both places (road access=False). The dependency is a logical one (no physical commodity flow).

Variable	Description	Dep. A	Dep. B	Dep. C
Source	Supporting CI component	Cell tower	Power line	Hospital
Target	Dependent CI component	Hospital	Cell tower	People-cluster
Distance Threshold	The maximum distance for establishing a link between two nodes is determined by a circle around the target with respective radius if road access is not required, else the shortest path via road edges connecting source and target nodes must not exceed the specified threshold	30 km	15 km	80 km
Redundancy	Whether a target node is connected to all CI nodes of type source within a specified distance threshold (redundancy = TRUE) or only to the single closest one (FALSE).	TRUE	FALSE	TRUE
Road Access	Whether a road path must exist between source and target.	FALSE	FALSE	TRUE
Flow	Whether the flow through the dependency edge is informed by a physically informed continuous variable (such as power cluster capacity), or is a pragmatic binary variable, indicating whether supply can be provided or not, based on the functional state of the source.	Logical	Physical	Logical

Second, for each combination of source-target pair *jk* for which edges e^{jk} were created in the interdependent CI graph, the attributes capacity C^{jk} and capacity threshold T^{jk} are assigned to all nodes. C^{ik} is initialized to discrete values, depending on whether a node is a source (1), a sink (-1) or neither (0) for the flow from CI network of type *j* to type *k*. T^{jk} ([0,1]) indicates what percentage of a standardized flow

unit from *j* needs to arrive at a component of type *k* for it to remain functional. This is illustrated in in Figure 2.2, panel A.1 (right): node #6 represents a hospital (h) which depends on electric power (e) and telecommunications (c), and provides healthcare services to people (p). Hence $C^{e,h}$ and $C^{c,h}$ =-1, while $C^{h,p}$=1. For the hospital to remain functional, it needs to receive at least 0.6 standardized units of power through its dependency link(s) ($T^{e,h}$=0.6), 1 unit of telecommunications access ($T^{c,h}$=1), and no unit of healthcare access, since it is the provider of this service ($T^{h,p}$=0).

2.1.4. Assigning Flows and Determining Functional States of Infrastructure Components

Incorporating commodity flows in addition to a system's topology, has been argued as crucial for capturing system performances adequately [33]. Yet, interdependent CI networks entail flows *within* individual networks (e.g. power in the power grid), and *across* networks (e.g. power to hospitals). Flows are furthermore of different natures, involving physical commodities (water, electricity, etc.) as well as logical dependencies (connectivity to mobile communications). To deal with this diversity, internal flows in CI networks and flows along dependencies between CI networks are treated separately. Results are then translated into binary functional states and normalized capacity values for coherence across all networks. Formally, those calculations are performed on subgraphs of the previously established interdependent CI graph *G,* henceforth denominated as G'^{j} and G'^{jk}. Subgraphs span all elements of infrastructure type *j,* and of types *j*, *k*, and linking edges e^{jk}, respectively, yet also retain their reference to the overaching graph *G*, which is hence updated. Figure 2.2, panel A.2 provides a visual illustration of such subgraphs.

Flows within networks For networks with internal flows between sources and sink elements, infrastructure type-specific flow assignment algorithms, flexibly tailored to the data and knowledge available, are employed to update all capacity attributes C^{jk} on the corresponding subgraphs G'^{j} (for examples on flow calculation approaches, see [47] for road networks, [48] for water networks and [49] for power networks). Figure 2.2, panel A.2 (left) illustrates this procedure for the power network, which is the only network involving internal commodity flows in this stylized example. In absence of further system knowledge apart from demand (per capita consumption data), supply (power plant generation data) and network topology, a cluster approach is employed. For each cluster in G'^{e} (here there is only one cluster), the ratio of supply (28 GWh) to demand (35 GWh) is computed, and assigned as a new relative capacity value $C^{e,k}$ (here 0.8) to all nodes in that cluster. This can be read as the power system operating at C*100% of its required capacity. Functional states *F* of the components remain unaltered in this mechanism.

Flows across networks The goal of this step is to determine the functionality *F* of each dependent infrastructure node in the interdependent CI graph based on the available capacities from other supporting infrastructure nodes. For each unique type of dependencies *jk* (e.g., power-communication, *j*=e, *k*=c) in *G*, subgraph G'^{jk} is extracted. A received supply variable M^{jk} is computed for each node in G'^{jk}. M^{jk} amounts to the sum of capacities C^{jk} received at target nodes *k* from functional source nodes *j* via an edge e^{jk}, and is hence 0 at nodes of type *j*. Technically, this flow propagation is computed on the adjacency matrix using matrix multiplication only, which is computationally efficient even for large networks. If M^{jk} is smaller than

a previously set capacity threshold T^{jk}, a node loses functionality (F=0). Figure 2.2, panel A.2 (right) illustrates this procedure formally (Eqs. (1) and (2)) and graphically on the electric power-mobile communications subgraph, which entails a physical, continuous variable flow, and on the mobile communications-healthcare subgraph, approximated by a binary (logic) variable flow: The cell tower node #7 receives a total of M^{ec} = 0.8 normalized units of power from the power sources it is connected to, which is greater than the capacity threshold (here set to T^{ec} = 0.6). It hence remains functional (F=1). Hospital node #1 receives M^{ch} = 2 logical units of supplies from both cell towers it is connected to. As this exceeds the needed (logical) units of cell tower supply (T^{ch}= 1), the hospital also remains functional (F=1).

Since dependency loops (inter-dependencies) can exist among CI networks, internal and inter-network flow assignment procedures are iteratively repeated untio there are no more functional variable changes across any elements in the interdependent CI graph G.

2.1.5. Determining Basic Service Access

The final step is to compute basic service access for a range of services at population nodes. Basic service access, according to the United Nation's definition[1], is ensured through the confluence of two factors:

i. *functionality* of the CI (component) responsible for the provision of a service
ii. a notion of *accessibility* to the CI (component)

Here, we define functionality through the functional states of the infrastructure graph elements. Accessibility is defined either through literal road path availabilty between end-user and infrastructure (e.g. hospitals for healthcare services) or through coverage of an area around an infrastructure's location (e.g. cell towers for mobile communication services). A qualitative summary of basic service access parametrizations for six services examined in this work is given in Table 2.3.

Table 2.3 Basic service access conditions implemented in the systems model.

Basic Service	Description
Healthcare	Existence of an intact road-path below a certain distance threshold to a functioning facility.
Education	Existence of an intact road-path below a certain distance threshold to a functioning facility.
Energy	Functional connection to an intact power cluster which runs above a certain capacity ratio.
Basic information services	Functional connection to an intact cell tower within a certain distance threshold.
Mobility	Functional connection to an intact road element within a certain distance threshold.
Basic drinking water services	Functional connection to an intact wastewater treatment plant within a certain distance threshold.

The quantitative basic service access algorithm is implemented in analogy to the flow assignment and functionality determination algorithm in the previous step. For each unique infrastructure-population pair combination *jp,* for which dependency edges e^{jp} exist in the interdependent CI graph G, the subgraph G'^{jp}

[1] Metadata repository to the SDGs for indicator 1.4.1 - Proportion of population living in households with access to basic services: "*Basic Services refer to public service provision systems that meet human basic needs including drinking water, sanitation, hygiene, energy, mobility, waste collection, health care, education and information technologies. […] Access to basic services implies that sufficient and affordable service is reliably available with adequate quality*."

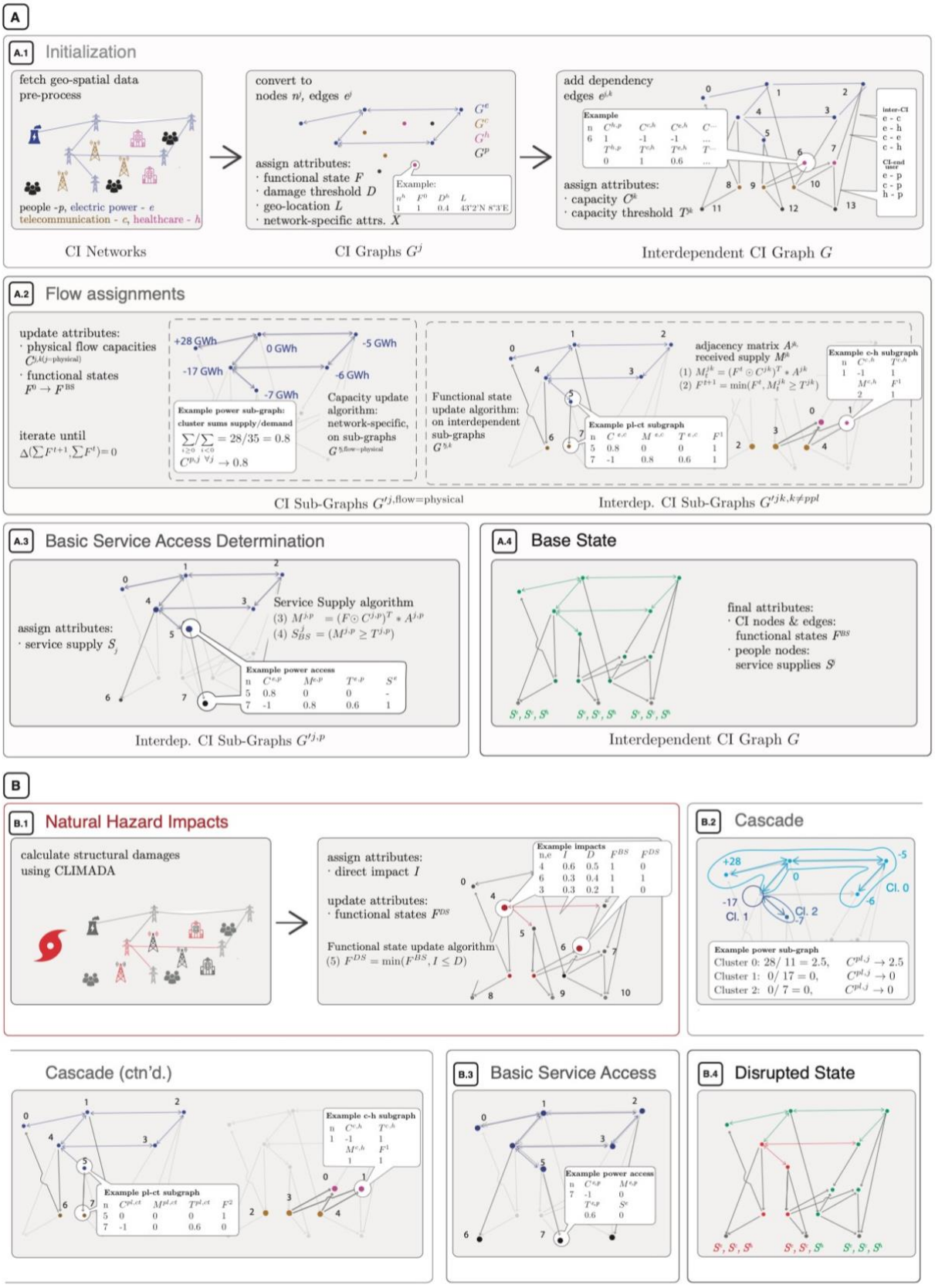

Figure 2.2 Technical implementation of the interdependent CI networks model, flow assignment / failure cascade algorithm and basic service access determination. Multi-panel A introduces terminology, crucial variables and formal algorithms on a stylized example featuring 3 CI networks and population. Multi-panel B shows how those introduced blocks of the modelling chain produce CI failure cascades and estimate service access disruptions due to structural damages caused by a natural hazard event. Detailed explanation is given in sections 2.1 - 2.4. For a list of abbreviations and formal treatment, see annex A.

spanning G'^{p}, G'^{j} and $e^{j,p}$ is extracted. Received services M^{jp} are hence computed as the sum of capacities from source infrastructure nodes arriving at population nodes (see eqs. 3 and 4 in Figure 2.2, panel A.3). Each population (target) node is then assigned a service attribute S^{j}, indicative of the service provided by CI type j. The service is accessible (S^{j}=1) if M^{jp} exceeds the capacity threshold T^{jp} *and*, additionally, fullfils the access conditions (c.f. Table 2-3), else S^{j}=0. While the coverage-based access conditions are implicitly accounted for through the (non-)existence of a dependency edge, the literal (road-access) condition is checked for explicitly in the interdependent CI graph *G* through a shortest path algorithm, calculating the distance of the path between population node and facility node. Figure 2.2, panel A.3 illustrates the procedure with the example of electric power access, where population node #7 receives M^{ep}=0.8 normalized units of power, which exceeds the capacity threshold (T^{ep}=0.6) and hence the service is accessbile (S^{e}=1).

The interdependent CI graph with functional state attributes *F* at infrastructure elements and service attributes *S* at population nodes hence defines the *base state.* Figure 2.2, panel A.4 illustrates this for the three infrastructure networks and the corresponding three service types at the population network (electric power access S^{e}, basic information access S^{c} and healthcare access S^{h}).

2.2. Stage II: Disaster Risk Model

While several platforms for natural hazard modelling exist, the open-source software CLIMADA (CLImate ADAptation) [45] is the only globally consistent multi-hazard platform that is openly and freely available to assess the impacts of natural hazards and for appraisal of adaptation options [50]. The event based modelling approach of CLIMADA has been used, among others, to conduct studies on the impacts of tropical cyclones on assets [51] and displaced people [52], on impacts from river floods [53], and in the wider context of Economics of Climate Adaptation studies [54]. The framework allows for a fully probabilistic risk assessment based on the IPCC risk definition as:

$$Risk = Hazard \times Exposure \times Vulnerability$$

Hazard is a spatially explicit representation of the disaster intensity (such as wind speed for storms, water height for floods). *Exposure* refers to the geo-referenced assets or people that are located in the area of interest. *Vulnerability* is an exposure-specific mapping of hazard intensity to expectable damage and also termed *impact function* or *fragility curve* in either of the communities. Since CLIMADA allows for modular, user-definable representations of exposure, vulnerability and hazard at any scale and resolution of choice, we tailor the engine to produce direct damage estimates to CI components. Vulnerability curves for desired hazard and CI component combinations can be taken from literature, such as the HAZUS technical manual provided by the US Federal Emergency Management Agency (FEMA) for several natural hazards. Hazards can be user-ingested raster or vector data and work off-the shelf for historical and probabilistic tropical cyclones in CLIMADA. CI component data is converted to a compatible CLIMADA exposure format by interpolating line and polygon shaped data to centroids, and re-aggregated into their original shape after

impact calculations. For instance, a tropical cyclone event may cause damages to power lines, cell towers or hospitals as illustrated in Figure 2.2, panel B.1 (left).

2.3. Stage III & IV: Impacts

2.3.1. Technical Impacts

For each element in the interdependent graph, the impact to the corresponding component computed with CLIMADA is assigned as attribute *I*. Functional state *F* of an element is set to zero if the impact *I* exceeds the damage threshold D^j as illustrated in Figure 2.2, panel B.1 (right).

This change in functional states can set off a failure cascade within the graph, through both internal and dependency-induced flow changes. In order to propagate the disruption, the capacities and functional attributes of all CI components are updated by applying the algorithm described in section 2.1.4 iteratively until a new steady state is obtained. In our example illustrated in Figure 2.2, panel B.2 several cascades occur: The power graph is split into three clusters as a consequence of the initial failure of a node and an edge element, whereby two clusters (Cl. 1 and Cl. 2) remain without capacity as they are cut off from connection to the power plant ($C^{e,k}$=0). Interdependencies among CI networks further propagate those disruptions (cell tower #7 is connected to a capacity-less power node, hence becoming dysfunctional; hospital #1 still receives 1 unit of supply - instead of previously 2 - from supporting cell towers, which prevents its failure).

2.3.2. Human-centric Impacts

Once CI component failures are determined, basic service access is re-computed as described in section 2.1.5. See illustration in Figure 2.2, panel B.3 for the given stylized example on population's power access, leading to a new, *disrupted state* (Figure 2.2, panel B.4)

2.4. Model Uncertainties and Sensitivity Testing

Due to the amount of consecutive stages featured in the presented modelling chain, model assumptions and representational choices in one stage may greatly influence end-results. In order to allow for evaluation of such sensitivities, Table 2.4 provides a brief discussion on the main points where model uncertainties are introduced.

Table 2.4 Drivers of model uncertainties throughout all stages in the modelling chain.

Stage	Source	Explanation
I	CI system representations	Choices on CI components included or excluded, simplifications (for instance, no differentiation between transmission lines of different voltages, approximating the communication network by cell towers, water network by water treatment plants)
	Dependency Identification	Choice of dependency rules (i.e., heuristics, between which CI systems dependencies exist)
	Dependency Parametrization	Choice of conditions for dependency establishment (i.e. distance thresholds between components identified through heuristics, path requirements, etc.)
II	Hazard Footprint	Resolution, spatial accuracy and representational validity, when in-or excluding sub-hazards (e.g. wind-fields, storm surge and torrential rainfall for tropical cyclones) or multi-hazard phenomena (compound events).
	Vulnerability Curves	Assumptions on (deterministic) relationship between hazard intensity and component damages.

	Damage-Functionality Thresholds	Assumptions on the (deterministic, threshold-based) relationship between structural damages and resulting component functionality levels.
III	Cascading algorithm	Deterministic (strict) propagation of failures along dependencies, assumption on target becoming strictly dysfunctional due to failure at source.
IV	End-user Dependencies	Uncertainties are analogous to stage I.
	Basic Service Parametrization	

Scenario analyses, where few of the parameters are varied within 'realistic' bounds at a time, can provide a qualitative way of identifying non-linearities in the system. This is readily achievable for parametrizations of dependency conditions, vulnerability curves and functional thresholds. Uncertainties in the failure trigger, i.e. the hazard footprint, can be mitigated by taking a probabilistic approach to hazard modelling, as for instance the tropical cyclone module offers in CLIMADA, where synthetic, slightly varied tracks can be generated from an original historic one. Representational choices, such as included CI components and dependencies, are mostly constrained by data and knowledge availability.

3. Results: CI Failures & Basic Service Disruptions from Hurricane Michael

Tropical Cyclone Michael made landfall in the Florida Panhandle on the 7th of October 2018, and caused severe impacts across Florida, Alabama and Georgia, both in terms of direct asset damages (over US$ 25 billions) and lives lost (at least 43) [5], as well as in terms of CI failures (power and mobile communication outages affecting millions, among others). It was selected for demonstration based on two reasons. Ample documentation of the event permits result validation and provides a reality check on quality and information content of the developed model. Further, Michael's severity was dominated by strong winds and storm surge as opposed to torrential rainfalls [55]. The hazard can therefore be approximated by modelling only its wind-field, lending itself as an illustrative, yet simple enough example.

3.1. Model demonstration

Stage I: Creating an Interdependent CI Network We delimit the system of study to the states of Florida, Alabama and Georgia which were directly hit by hurricane-strength winds. Besides population count data, infrastructures types considered are main roads, transmission power lines, power plants, cell towers, wastewater treatment plants, healthcare institutions and public schools. For details on data pre-processing and data sources, see annex sections 0. Figure 3.1 column 'CIs' displays the CI networks. For the power network, supply sources and demand sinks could be located and quantified drawing on power plant generation and energy consumption statistics (see annex C.1). To generate the interdependent CI graph, sixteen distinct dependencies were identified in between CI networks and between CI networks and population, and parametrized as indicated in annex C.1. The established interdependent CI graph consists of 78'568 nodes and 483'123 edges, dependencies making up 59% of all edges (see 0 for a detailed graph description). In this pre-disaster configuration (the base state), all components of the interdependent CI

graph are functional. Physical supply and demand are matched in the power sub-network and all other logical dependencies between different CI types are satisfied. Basic service access rates among the population amount to >99% for all service types considered (access to mobility, power, education, healthcare, mobile communications and drinking water).

Stage II: Tropical Cyclone Damage Calculations Track data for tropical cyclone Michael is obtained from IBTrACs. The wind field is computed from the CLIMADA tropical cyclone module, according to the parametrization in [56] (see 0); CI-type specific wind impact functions are taken from literature (ibid.) for all infrastructures except power plants, which are not designed to fail. Exposure layers are generated from geospatial information of the CI networks; line-shaped data (power lines, roads) is interpolated to points. Structural damages are computed using the CLIMADA impact module, results are displayed in Figure 3.1, column 'component damages'. Structural damage fractions are converted into component failures by applying a step function, which is, in absence of better knowledge, arbitrarily set at damage fractions of 30% and higher (see Figure 3.1, 'CI failures' where color-coded as "dysfunctional").

Stage III: CI Failure Cascades Structural component failures can trigger both internal failure cascades (i.e. within an individual CI network) and failure cascades across CI types, along dependencies. Under the given system specifications, only the power network features an internal cascading mechanism, as it contains designated source nodes (power plant), sink nodes (power line nodes with customer demands) and transition nodes (all other power line nodes). A cluster approach was chosen to capture this failure behaviour, where all components in a remaining functional cluster become dysfunctional once generation capacity falls below a certain fraction of demand (here set arbitrarily to 60%). Dependency-induced failure cascades are experienced across all CI networks within the interdependent graph. Results are displayed in Figure 3.1, 'CI failures', where cascaded failures are marked in the colour code.

Stage IV: Basic Service Disruptions To compute received services at population nodes, component functionality of the respective service-providing infrastructures along infrastructure-population dependency edges are checked, and road path availability and travel distance are re-calculated for those services requiring physical access (education and healthcare, here set to a maximum of 30 km and 100 km, resp.). Figure 3.1, 'Basic Service Access' shows the disruption results for access to mobility, power, healthcare, education, mobile communication and drinking water.

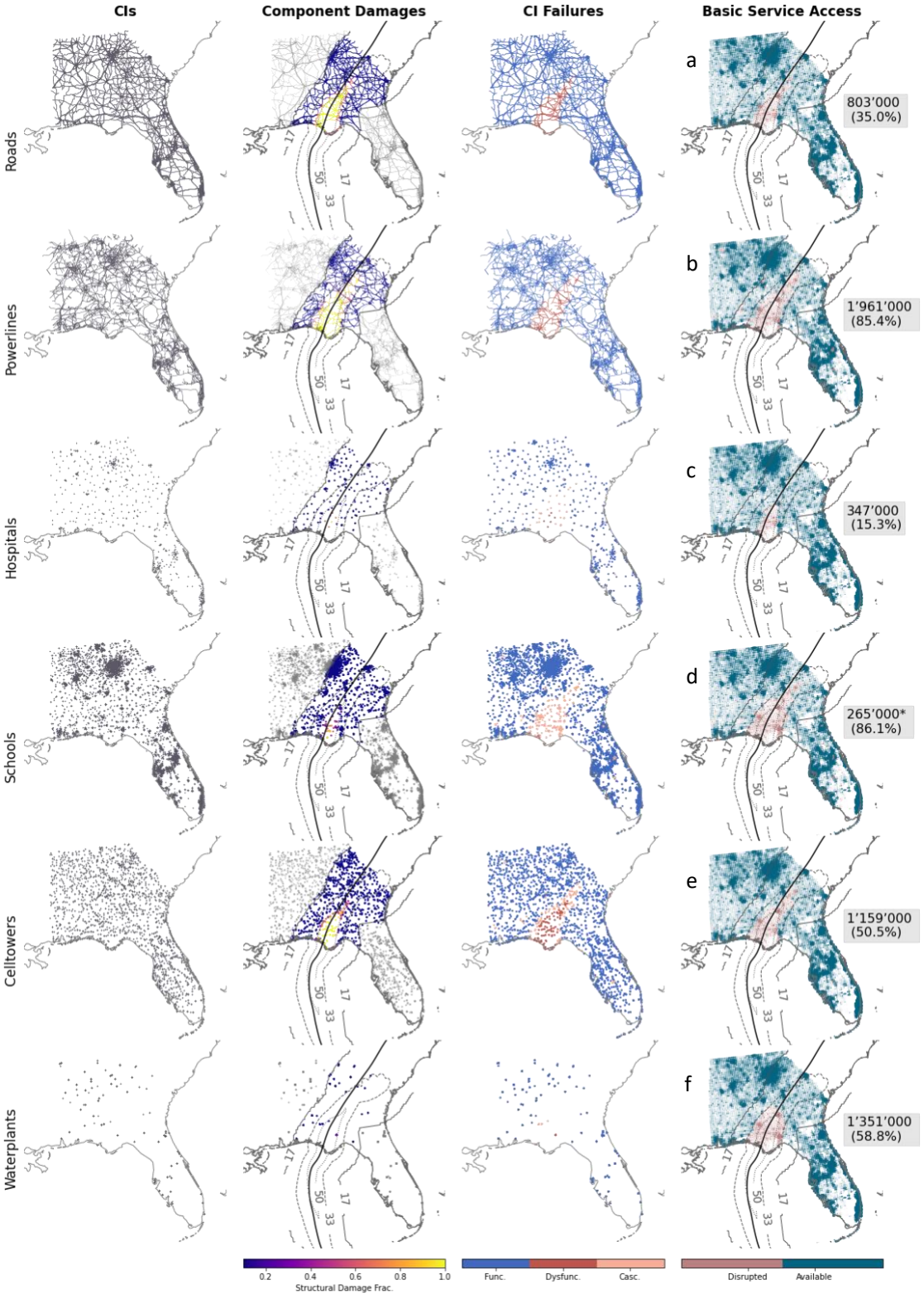

*Figure 3.1 From natural hazard to basic service disruptions in four stages. Demonstration for Hurricane Michael '18 hitting the Florida Panhandle: Asset data for 6 CIs across FL, AL & GA used in the CI model (column 'CIs'), wind-induced structural damages calculated with CLIMADA ('Component Damages'), CI failure cascades triggered by the initial disruption, resulting in functional, dysfunctional and cascaded dysfunctional components ('CI failures'), population impacted from basic service disruptions following CI failures ('Basic service access', a: access to mobility, b: power, c: healthcare, d: education, e: mobile communication, f: drinking water. Absolute numbers refer to calculations on impacted people, percentages are in relation to the total population exposed to TC-strength winds (>34 m/s)). *absolute number corrected by fraction of people enrolled in preK-12; (13.4%). TC track and wind-field contour lines are plotted in columns 2 & 4 for reference.*

3.2. Sensitivity Analysis

To study result sensitivity to assumptions along the modelling chain, seven scenarios (see Table C.4) are constructed to test the role of interdependencies and of parametrization decisions for impact functions and for functionality thresholds on result outcomes. The above presented case, referred to as 'base scenario' henceforth, is taken as a reference.

Results are greatly influenced by the inclusion of CI interdependencies: As cascaded failures account for a significant part of all infrastructure failures in the base scenario, the removal of this impact driver drastically reduces component failures across all CI types but roads, with strong consequences for projections of service disruptions. Numbers of affected people decrease by a factor of 2-6 for all basic services apart from access to mobility (see Figure 3.2, grey and annex Table C.5 for numeric results). While the inclusion of dependencies itself plays a great role in determining the magnitude of impacts, the exact parametrizations of establishment conditions thereof (such as distance thresholds, etc.) affect end results less strongly (cf. Table C.5).

Parametrization of impact functions directly influences estimates of structural damages, which has far-reaching consequences on the entire impact chain from immediate CI failures over cascades to basic service disruptions. Shifting impact functions by 15 m/s in either direction compared to the base scenario (i.e. same level of structural damage at wind intensities of 15 m/s more or less, resp.) can lead to a divergence in services disruption estimates between millions of people and none (see Figure 3.2 blues and annex Table C.5). Due to the resolution of the hazard footprint (360 arcsec, ca. 11 km), which exceeds most CI component lengths, results were less sensitive to the assumptions on the relationship between structural damages and functional performance of components, since components are mostly entirely affected or not at all (see Table C.5). This may change and become increasingly important, though, at higher hazard resolutions.

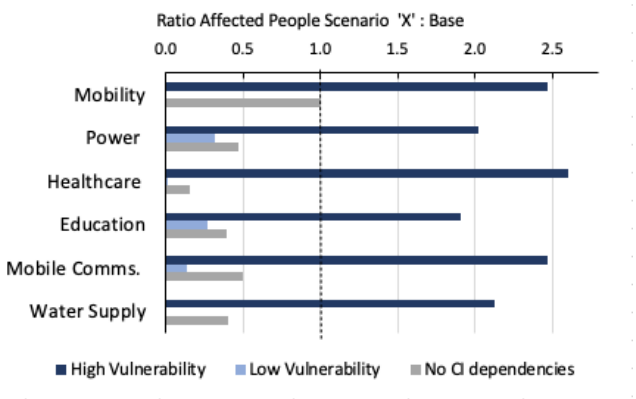

Figure 3.2 People affected by basic service disruptions for three scenarios, relative to base scenario presented in section 3.1. Grey: No CI-interdependencies, light-blue: low CI-component vulnerability (impact functions shifted towards higher wind-intensities), dark-blue: high CI component vulnerability (impact functions shifted toward lower intensities). For numerical results see Table C.5.

3.3. Validation

The aim of this validation is to collect evidence on whether the showcased impact cascades - from CI damages to affected people - *do* happen, and whether predicted impacts, even when drawing on coarse assumptions and a set of heuristics, are in the right order of magnitude. The multiple impact stages calculated within the underlying approach are reflected in the breadth of validation sources taken into account, and span official government releases, utility providers' reports and newspaper articles (see annex C.3 for a comprehensive overview).

Even for the case study region, where reporting after disasters is ample and well accessible, documentation on the entire disaster cascade is incomplete: structural damages are only incidentally reported across all infrastructure types, comprehensive functional outage reports are limited to the power and telecommunication sector, while accounts on basic service disruptions remain anecdotal. Figure 3.3 synthesizes this evidence, contrasting quantitative outage statistics against model outputs (panels b and e for power and telecom), and mapping qualitative service-related incidents against areas of modelled access disruptions (panels a, c, d and f for healthcare, education, mobility and drinking water).

Loss of power access is captured well, both in terms of impacted people (~1.65 million reported vs. 1.96 million modelled), and in terms of spatial distribution (compare Figure 3.3 and Figure 3.1 (a) for a more detailed visual reference). Loss of mobile communication access is not reported as such, yet documented occurrences of cell site outages coincide well with spatial model predictions on failed cell towers (see Figure 3.3 (e), aggregated at county level); most county predictions lie well within a 50% margin of error, even though the impact severity is overestimated in hurricane-hit counties located further inland.

Documented incidents related to the loss of healthcare access and healthcare infrastructure damages (i.e. hospital evacuations and structural damages, fatalities due to untimely care, etc.) coincide particularly well with the area where the model predicts disruptions (Figure 3.3 (c)). Equally for all other services, all reported incidents lie within the modelled area of concern. Yet, road damages and mobility-related incidents were reported far less inland than model predictions (Figure 3.3 (a)), as is the case with access to education (Figure 3.3 (d)) and most drastically with evidence on drinking water issues (Figure 3.3 (f)).

The divergence in projected and actual disruptions to mobility confirms the importance of choosing adequate impact functions, as pointed out also in the sensitivity analysis section. The impact function used in this study was designed for road disruptions from tree blow-down, which is prone to provide an overly pessimistic picture on (longer-lasting) structural damages.

Validation results for healthcare, education and power access highlight the importance of incorporating dependencies and failure cascade into the model, yet also show caveats of adequate parametrization:

Several hospitals which were not directly damaged, reported evacuations due to water and power supply issues, while many of the reported indirect deaths were linked to either patients or emergency workers not getting physical access to healthcare facilities in time. The good model performance in projecting

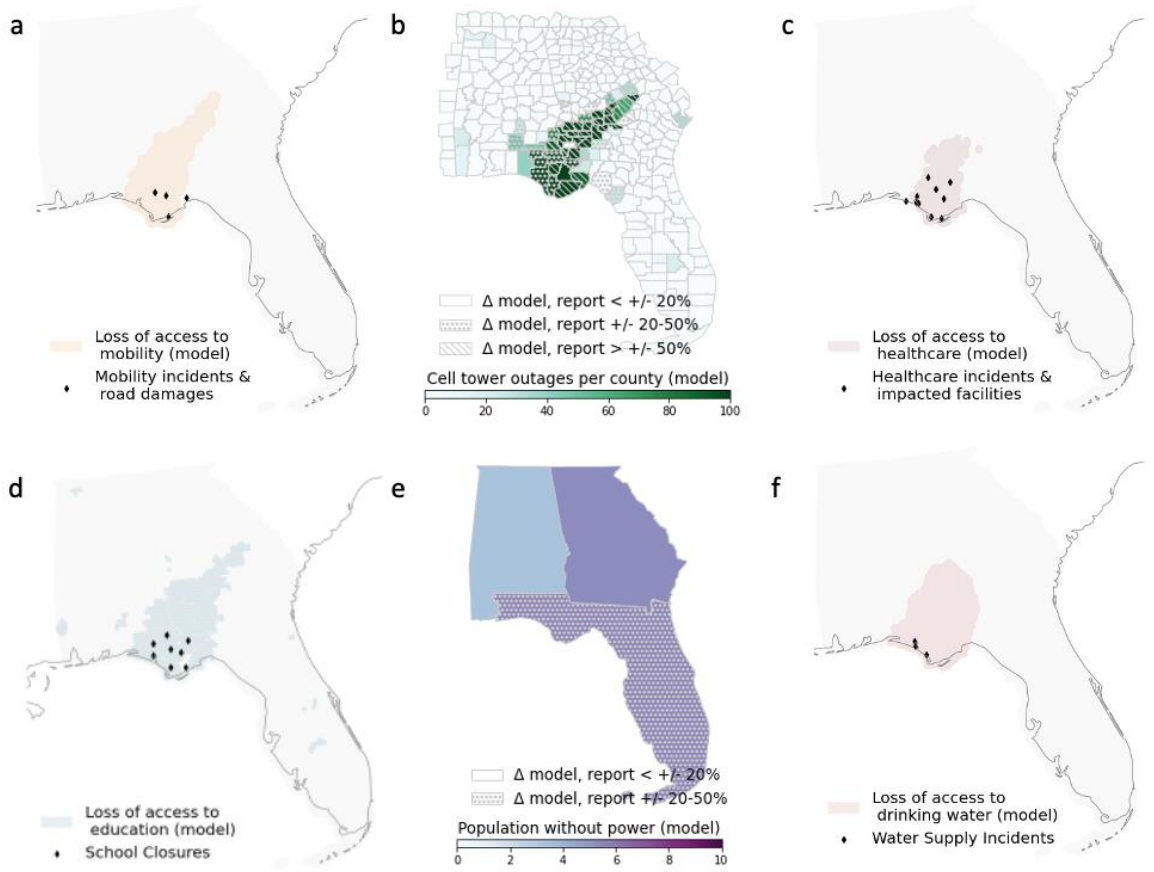

Figure 3.3 Validation results for power outages (a), cell site outages (b), water supply issues (c), healthcare-access related incidents and hospital damages (d), road blockages, structural damages and mobility incidents (e) and school closures (f).

healthcare disruptions is partly due to the adequate capturing of exactly those CI dependencies and the incorporation of road access conditions for the population, which are confirmed to be critical factors.

Similarly, the quite accurate projection of people affected by power outages could not have been reproduced without CI interdependencies, as the sensitivity analysis showed above. The choice of dependency specifications, however, also led to poor projections of disruptions to education access. The estimated 45'000 students reported to be missing school due to closures [2] fall short of the 265'000 projected by the model. This is partly due to the stricter dependency between end-users and educational facilities than between end-users and healthcare facilities: People are assigned to one fixed school, while any functional hospital within reach can be chosen. Contrary to failed hospitals, failed schools will therefore always cause disruptions in education access throughout the entire assignment surroundings, and damage over-estimations to such facilities will have larger consequences.

Lastly, the case of water access disruptions, which were more contained in reality than in model projections, demonstrates how the degree of system simplification may become problematic: In absence of better data, the drinking water system was proxied by water treatment plants only. As a consequence, the model projected large areas of disruption from a single failing facility, which seems not to be the behaviour observed in those real-world water systems.

Despite the fact that some service disruptions were less extensive than modelled, the integration of a hazard model and a CI model based on relatively simple dependency heuristics and readily available open-source data allowed to capture important failure dynamics within one interoperable calculation chain. The model reproduces impacts in the correct order of magnitude, allows to trace back impact drivers to parametrization decisions in each stage of the impact cascade, and to re-calibrate mechanisms. It further gives a social dimension to technical CI failures, mapping out areas of disruption for basic services which are not consistently monitored by official sources. While those are promising features, there is demand for an even more refined picture, as remarked by a reporter in the aftermath of TC Michael: "While the coastal devastation has become obvious, some disaster experts are most concerned about the conditions farther inland. (…) These are some of the most socially vulnerable places in the entire country, low-income counties with high proportions of older adults, and many people with disabilities and chronic illnesses" [57].

4. Discussion

The developed modelling framework was designed for interoperability, transferability and scale. Interoperability is achieved though the embedding of an infrastructure system model into the risk assessment platform CLIMADA, allowing for a streamlined workflow from natural hazards to social impacts. The linkage to an event-based hazard simulation engine is a way forward from the use of stylized polygons in absence of physically-informed hazard footprints [25], [58], hypothetical events [24] or return period maps which are not representative of individual events [59]. Transferability is ensured both theoretically and practically: While we provide readily available suggestions on infrastructure and population data sources, dependency heuristics and hazard models, the framework could handle both proprietary and/or other open-source data (e.g. regional or national-level developed data). This allows to investigate other infrastructure types, hazards, dependencies and case study regions of interest to the user. The scale criterion is integrated in the design of the infrastructure system model, which requires few technical specifications, and relies mainly on network topology and a set of heuristics for dependency and flow assignment procedures, enabling the study of large systems.

The results simulated must be interpreted as a first indicator on impact hotspots and peak disruptions from the angle of people at risk. The simplifying nature of network-based approaches has been recognized earlier as a necessary trade-off against capturing large system scales at which disasters can occur [18], [22]. The merit of the developed system model's approach therefore lies in the possibility of working at a globally consistent basis with several interdependent CI systems, yet does not replace specialized system models [33], [48], [49], [60] for detailed local analyses and individual infrastructure system optimizations.

The three information levels on infrastructure risk which the model provides (structural component damages, failure cascades, and service disruptions), align well with the highly diverse nature of real-world impact data, which is often anecdotal and encompasses several of those risk layers. This offers the versatility to calibrate and adjust parameters in the model based on evidence, such as tailoring impact

functions to match print media coverage on structural damages, or amending dependency heuristics to fit utility provider's outage reports. To the best of our knowledge, only few quantitative modelling studies [61] incorporate such feedback possibility. Obtaining results on direct and cascades infrastructure failures further allows to quantify the role of infrastructure dependencies in causing wide-spread impacts: Validation in the presented case study empirically confirmed that the extent of observed impacts could not be reproduced without the inclusion of dependencies between infrastructure networks, which is in line with findings from other research on infrastructure interdependencies [62], [63].

The sensitivity analysis highlighted that stuctural damage functions and dependency parametrizations are sources of considerable uncertainties in the model. Quantification of dependencies and their variable 'coupling strengths' [14] is ongoing research. The current use of capacities, capacity thresholds, redundancies and road-path availability checks in the parametrization of infrastructure dependencies is a first attempt to capture those and refine commonly employed user-assignment procedures relying purely on geospatial conditions (e.g. Voronoi tessellations) or on shortest path algorithms without alternative targets [21], [34], [64]. Yet, modelling of back-ups for failing dependencies (such as generator availability for power-dependent components [61]) and changing demand patterns for infrastructure-related services among end-users as a reaction to disaster occurrences [65], [66] may be improvements to the currently implemented cascading dynamics. Furthermore, the threshold approach employed to relate structural damages to loss of component functionality is a simplification for the notoriously challenging task of developing consistent performance indicators [67], for which research in the engineering community may lead to improved insights in the future.

Our approach only implicitly includes a notion of time. Since modelled structural damages to infrastructures need to surpass a certain threshold for the components to become dysfunctional, this implies that the model does not capture very minor disruptions. Yet, absence of an explicit time component hampers judgement of impact severity, which is a function of time [68]: While for healthcare access a few hours of disruptions in the immediate aftermath of disaster may be extremely relevant, they may be less so for access to schools, especially if occurring on a weekend. Introducing time could further provide an informative indication on restoration and recovery dynamics [69], [70] when introducing repair times and 'snapshots' of the interdependent CI network at various moments.

Lastly, our estimates of post-disaster basic service disruptions add an often-neglected human-centric dimension to the discourse on infrastructure risks [71], which both academic models, utility providers or government post-disaster reports do not usually capture systematically (cf. [43] as a rare exception); the holisitic approach further allows to include under-represented sectors in CI research such as healthcare [44] and education. This can offer valuable information to emergency responders with limited resources, and decision makers facing multi-criteria investment decisions alike [43], [71], [72]. However, and especially as research on social vulnerability is still in its infancy [41], it will be important to take a closer look at the differential impacts of basic service losses on different parts of the population, such as the poor,

the elderly or non-native speakers, which have repeatedly been shown to dispose of fewer coping mechanisms [15], [73].

5. Conclusion

Critical infrastructures such as powerlines, roads, telecommunication and healthcare systems across the globe are more exposed than ever to the risks of extreme weather events in a changing climate. CI failure models often operate at local scales with high data requirements and low transferability, focussing on the technical performance side. Natural hazards are often not explicitly modelled as a disruptive scenario therein. Natural hazard models, in turn, frequently focus on direct damages to assets, which neglect the networked and interdependent character inherent to critical infrastructure systems.

To bridge those gaps between infrastructure modellers and disaster risk modellers, we draw on well-established methods in both communities to develop an interoperable, coherent and open-source modelling framework for assessing spatially explicit, large-scale risks from infrastructure failure cascades and their social impacts induced by natural hazards. Embedded into the risk assessment platform CLIMADA, a state-of-the-art tool for natural hazard impact calculations and adaptation options appraisal, we demonstrate a network theory-based infrastructure systems model designed to require few technical details apart from commonly available asset location and population data, which can handle many types of infrastructure networks and captures interdependencies among them based on a set of heuristics. The framework hence offers a three-layered view on infrastructure risks in terms of on infrastructure component damages, technical failure cascades, and human-centric basic service disruptions. It is readily transferrable across geographies, and can be tailored to include CI systems, interdependencies and hazards of interest to the user.

The validated case study on Hurricane Michael across the US states of Florida, Georgia and Alabama for six interdependent CI networks showed that the established modelling chain captures impact hotspots and reproduces failure cascade dynamics, which could not be obtained when looking at structural infrastructure damages alone. It also showed how real-world impact data, such as outage reports and print-media accounts, can be used to iteratively refine and calibrate the model. Projecting spatially explicit locations of service disruptions experienced by the dependent population as a result of infrastructure failures further adds a novel layer of risk information, which is usually not available on the ground.

While we do not offer the one single "comprehensive methodological approach with a platform of linked models and data interoperability for modelling infrastructure interdependencies for a range of different stakeholder concerns and decision contexts" [71] our approach takes a step into this direction. We provide a tool apt for decision making-contexts involving large geographic scope and the effects of several interdependent CI systems' responses to disruptions for the population: The global consistency of the approach permits a comparative view of risk across countries, relevant for international policy frameworks; adaptation planning and infrastructure investments for resilience can be evaluated under their aversion potential for different types of human-centric impacts and under trade-offs amongst different CI sectors; post-disaster hotspot analyses can lead to more targeted humanitarian relief and recovery activities.

Acknowledgements

This project has received funding from the European Union's Horizon 2020 research and innovation programme under grant agreement No 821010 and under grant agreement No 820712. Elco Koks was further supported by the Netherlands Organisation for Scientific Research (NWO; grant no. VI.Veni.194.033).

Data Availability

CLIMADA risk assessment platform is accessible on GitHub (https://github.com/CLIMADA-project/climada_python, https://github.com/CLIMADA-project/climada_petals). Code for case study results and figures is accessible under https://github.com/CLIMADA-project/climada_papers. All raw data sources needed for reproducing calculations are mentioned in the text and annex.

References

[1] E. Zio, "Challenges in the vulnerability and risk analysis of critical infrastructures," *Reliability Engineering & System Safety*, vol. 152, pp. 137–150, Aug. 2016, doi: 10.1016/j.ress.2016.02.009.

[2] W. T. Price and C. Glenn, "Schools closed across the Panhandle, 45,000 kids missing class due to Hurricane Michael," *Pensacola News Journal*, Oct. 17, 2018. Accessed: Jan. 25, 2022. [Online]. Available: https://www.pnj.com/story/news/2018/10/17/hurricane-michael-closes-schools-florida/1660289002/

[3] Bay District Schools, "Hurricane Michael Recovery Information." https://www.bay.k12.fl.us/hurricane-michael (accessed Jan. 25, 2022).

[4] J. Burlew, "43 and counting: Deconstructing the Florida death toll after Hurricane Michael," *Tallahassee Democrat*, Nov. 29, 2018. Accessed: Jan. 25, 2022. [Online]. Available: https://www.tallahassee.com/story/news/2018/11/29/43-and-counting-deconstructing-death-toll-hurricane-michael/2124902002/

[5] J. L. Beven II, Robbie Berg, and Andrew Hagen, "Hurricane Michael Tropical Cyclone Report," National Hurricane Center, AL142018, May 2019. Accessed: Jan. 25, 2022. [Online]. Available: https://www.nhc.noaa.gov/data/tcr/AL142018_Michael.pdf

[6] S. Thacker *et al.*, "Infrastructure for sustainable development," *Nature Sustainability*, vol. 2, no. 4, Art. no. 4, Apr. 2019, doi: 10.1038/s41893-019-0256-8.

[7] McKinsey Global Institute, "Climate risk and response. Physical hazards and socioeconomic impacts.," Jan. 2020. https://www.mckinsey.com/~/media/mckinsey/business%20functions/sustainability/our%20insights/climate%20risk%20and%20response%20physical%20hazards%20and%20socioeconomic%20impacts/mgi-climate-risk-and-response-full-report-vf.pdf (accessed Jun. 24, 2020).

[8] A. N. Yesudian and R. J. Dawson, "Global analysis of sea level rise risk to airports," *Climate Risk Management*, vol. 31, p. 100266, Jan. 2021, doi: 10.1016/j.crm.2020.100266.

[9] E. E. Koks *et al.*, "A global multi-hazard risk analysis of road and railway infrastructure assets," *Nature Communications*, vol. 10, no. 1, Art. no. 1, Jun. 2019, doi: 10.1038/s41467-019-10442-3.

[10] C. Nicolas *et al.*, "Stronger Power: Improving Power Sector Resilience to Natural Hazards," World Bank, Washington, DC, Jun. 2019. doi: 10.1596/31910.

[11] Thacker S. *et al.*, “Infrastructure for climate action,” UNOPS, Copenhagen, Denmark., 2021. Accessed: Nov. 26, 2021. [Online]. Available: https://www.unops.org/news-and-stories/news/infrastructure-for-climate-action
[12] “Sendai Framework for Disaster Risk Reduction 2015-2030,” UNDRR, 2015. Accessed: Nov. 26, 2021. [Online]. Available: https://www.undrr.org/publication/sendai-framework-disaster-risk-reduction-2015-2030
[13] “SWD(2013)318 - COMMISSION STAFF WORKING DOCUMENT on a new approach to the European Programme for Critical Infrastructure Protection Making European Critical Infrastructures more secure,” European Commission, 2013. Accessed: Nov. 11, 2020. [Online]. Available: https://ec.europa.eu/transparency/regdoc/?fuseaction=list&coteId=10102&year=2013&number=318&version=ALL&language=en
[14] S. M. Rinaldi, J. P. Peerenboom, and T. K. Kelly, “Identifying, understanding, and analyzing critical infrastructure interdependencies,” *IEEE Control Systems Magazine*, vol. 21, no. 6, pp. 11–25, Dec. 2001, doi: 10.1109/37.969131.
[15] D. Mitsova, A.-M. Esnard, A. Sapat, and B. S. Lai, “Socioeconomic vulnerability and electric power restoration timelines in Florida: the case of Hurricane Irma,” *Nat Hazards*, vol. 94, no. 2, pp. 689–709, Nov. 2018, doi: 10.1007/s11069-018-3413-x.
[16] ECA Working Group, “Shaping Climate-Resilient Development – A Framework for Decision-Making,” 2009. Accessed: Jun. 05, 2020. [Online]. Available: https://ethz.ch/content/dam/ethz/special-interest/usys/ied/wcr-dam/documents/Economics_of_Climate_Adaptation_ECA.pdf
[17] Stip, C., Z. Mao, G. Browder, L. Bonzanigo, and J. Tracy, “Water Infrastructure Resilience – Examples of Dams, Wastewater Treatment Plants, and Water Supply and Sanitation Systems,” World Bank, Washington, DC, Sector note for LIFELINES: The Resilient Infrastructure Opportunity, 2019. [Online]. Available: http://documents1.worldbank.org/curated/en/960111560794042138/pdf/Water-Infrastructure-Resilience-Examples-of-Dams-Wastewater-Treatment-Plants-and-Water-Supply-and-Sanitation-Systems.pdf
[18] S. Hallegatte, J. Rentschler, and J. Rozenberg, *Lifelines: The Resilient Infrastructure Opportunity*. World Bank Publications, 2019.
[19] D. N. Bresch, J. Berghuijs, R. Egloff, and R. Kupers, “A Resilience Lens for Enterprise Risk Management,” in *Turbulence: A Corporate Perspective on Collaborating for Resilience*, Amsterdam University Press, 2014, pp. 49–65. Accessed: Jun. 08, 2020. [Online]. Available: https://www.research-collection.ethz.ch/handle/20.500.11850/127039
[20] R. J. Dawson *et al.*, “A systems framework for national assessment of climate risks to infrastructure,” *Philosophical Transactions of the Royal Society A: Mathematical, Physical and Engineering Sciences*, vol. 376, no. 2121, p. 20170298, Jun. 2018, doi: 10.1098/rsta.2017.0298.
[21] R. Pant, J. W. Hall, and S. Thacker, “System-of-systems framework for global infrastructure vulnerability assessments,” 2017. Accessed: Nov. 03, 2020. [Online]. Available: https://www.greengrowthknowledge.org/sites/default/files/downloads/resource/System-of-systems%20framework%20for%20global%20infrastructure%20vulnerability%20assessments.pdf
[22] M. Ouyang, “Review on modeling and simulation of interdependent critical infrastructure systems,” *Reliability Engineering & System Safety*, vol. 121, pp. 43–60, Jan. 2014, doi: 10.1016/j.ress.2013.06.040.
[23] E. E. Lee, J. E. Mitchell, and W. A. Wallace, “Network Flow Approaches for Analyzing and Managing Disruptions to Interdependent Infrastructure Systems,” in *Wiley Handbook of Science and Technology for Homeland Security*, American Cancer Society, 2009, pp. 1–9. doi: 10.1002/9780470087923.hhs686.
[24] R. A. Loggins and W. A. Wallace, “Rapid Assessment of Hurricane Damage and Disruption to Interdependent Civil Infrastructure Systems,” *Journal of Infrastructure Systems*, vol. 21, no. 4, p. 04015005, Dec. 2015, doi: 10.1061/(ASCE)IS.1943-555X.0000249.
[25] C. Zorn, R. Pant, S. Thacker, and A. Y. Shamseldin, “Evaluating the Magnitude and Spatial Extent of Disruptions Across Interdependent National Infrastructure Networks,” *ASME J. Risk Uncertainty Part B*, vol. 6, no. 2, Jun. 2020, doi: 10.1115/1.4046327.
[26] R. Pant, S. Thacker, J. W. Hall, D. Alderson, and S. Barr, “Critical infrastructure impact assessment due to flood exposure,” *Journal of Flood Risk Management*, vol. 11, no. 1, pp. 22–33, 2018, doi: 10.1111/jfr3.12288.
[27] R. Pant, J. W. Hall, and S. P. Blainey, “Vulnerability assessment framework for interdependent critical infrastructures: case-study for Great Britain’s rail network,” *European Journal of Transport and Infrastructure Research*, vol. 16, no. 1, Art. no. 1, Jan. 2016, doi: 10.18757/ejtir.2016.16.1.3120.
[28] N. Goldbeck, P. Angeloudis, and W. Y. Ochieng, “Resilience assessment for interdependent urban infrastructure systems using dynamic network flow models,” *Reliability Engineering & System Safety*, vol. 188, pp. 62–79, Aug. 2019, doi: 10.1016/j.ress.2019.03.007.
[29] C. Nan and G. Sansavini, “A quantitative method for assessing resilience of interdependent infrastructures,” *Reliability Engineering & System Safety*, vol. 157, pp. 35–53, Jan. 2017, doi: 10.1016/j.ress.2016.08.013.
[30] L. Dueñas-Osorio, J. I. Craig, and B. J. Goodno, “Seismic response of critical interdependent networks,” *Earthquake Engineering & Structural Dynamics*, vol. 36, no. 2, pp. 285–306, 2007, doi: 10.1002/eqe.626.
[31] J. Banerjee, K. Basu, and A. Sen, “Analysing robustness in intra-dependent and inter-dependent networks using a new model of interdependency,” *International Journal of Critical Infrastructures*, vol. 14, no. 2, pp. 156–181, Jan. 2018, doi: 10.1504/IJCIS.2018.091938.
[32] M. Ouyang and L. Dueñas-Osorio, “An approach to design interface topologies across interdependent urban infrastructure systems,” *Reliability Engineering & System Safety*, vol. 96, no. 11, pp. 1462–1473, Nov. 2011, doi: 10.1016/j.ress.2011.06.002.

[33] R. Guidotti, H. Chmielewski, V. Unnikrishnan, P. Gardoni, T. McAllister, and J. van de Lindt, "Modeling the resilience of critical infrastructure: the role of network dependencies," *Sustainable and Resilient Infrastructure*, vol. 1, no. 3–4, pp. 153–168, Nov. 2016, doi: 10.1080/23789689.2016.1254999.
[34] S. Thacker, R. Pant, and J. W. Hall, "System-of-systems formulation and disruption analysis for multi-scale critical national infrastructures," *Reliability Engineering & System Safety*, vol. 167, pp. 30–41, Nov. 2017, doi: 10.1016/j.ress.2017.04.023.
[35] H. Masoomi, H. Burton, A. Tomar, and A. Mosleh, "Simulation-Based Assessment of Postearthquake Functionality of Buildings with Disruptions to Cross-Dependent Utility Networks," *Journal of Structural Engineering*, vol. 146, no. 5, p. 04020070, May 2020, doi: 10.1061/(ASCE)ST.1943-541X.0002555.
[36] X. He and E. J. Cha, "Modeling the damage and recovery of interdependent civil infrastructure network using Dynamic Integrated Network model," *Sustainable and Resilient Infrastructure*, vol. 5, no. 3, pp. 152–167, May 2020, doi: 10.1080/23789689.2018.1448662.
[37] I. Hernandez-Fajardo and L. Dueñas-Osorio, "Probabilistic study of cascading failures in complex interdependent lifeline systems," *Reliability Engineering & System Safety*, vol. 111, pp. 260–272, Mar. 2013, doi: 10.1016/j.ress.2012.10.012.
[38] D. Z. Tootaghaj, N. Bartolini, H. Khamfroush, T. He, N. R. Chaudhuri, and T. L. Porta, "Mitigation and Recovery From Cascading Failures in Interdependent Networks Under Uncertainty," *IEEE Transactions on Control of Network Systems*, vol. 6, no. 2, pp. 501–514, Jun. 2019, doi: 10.1109/TCNS.2018.2843168.
[39] H. Fotouhi, S. Moryadee, and E. Miller-Hooks, "Quantifying the resilience of an urban traffic-electric power coupled system," *Reliability Engineering & System Safety*, vol. 163, pp. 79–94, Jul. 2017, doi: 10.1016/j.ress.2017.01.026.
[40] J. Beyza, H. F. Ruiz-Paredes, E. Garcia-Paricio, and J. M. Yusta, "Assessing the criticality of interdependent power and gas systems using complex networks and load flow techniques," *Physica A: Statistical Mechanics and its Applications*, vol. 540, p. 123169, Feb. 2020, doi: 10.1016/j.physa.2019.123169.
[41] M. Garschagen and S. Sandholz, "The role of minimum supply and social vulnerability assessment for governing critical infrastructure failure: current gaps and future agenda," *Natural Hazards and Earth System Sciences*, vol. 18, no. 4, pp. 1233–1246, Apr. 2018, doi: https://doi.org/10.5194/nhess-18-1233-2018.
[42] S. E. Chang, T. L. McDaniels, J. Mikawoz, and K. Peterson, "Infrastructure failure interdependencies in extreme events: power outage consequences in the 1998 Ice Storm," *Nat Hazards*, vol. 41, no. 2, pp. 337–358, May 2007, doi: 10.1007/s11069-006-9039-4.
[43] D. B. Karakoc, K. Barker, C. W. Zobel, and Y. Almoghathawi, "Social vulnerability and equity perspectives on interdependent infrastructure network component importance," *Sustainable Cities and Society*, vol. 57, p. 102072, Jun. 2020, doi: 10.1016/j.scs.2020.102072.
[44] S. E. Chang, C. Pasion, S. Yavari, and K. Elwood, "Social Impacts of Lifeline Losses: Modeling Displaced Populations and Health Care Functionality," pp. 1–10, Apr. 2012, doi: 10.1061/41050(357)54.
[45] G. Aznar-Siguan and D. N. Bresch, "CLIMADA v1: a global weather and climate risk assessment platform," *Geoscientific Model Development*, vol. 12, no. 7, pp. 3085–3097, Jul. 2019, doi: 10.5194/gmd-12-3085-2019.
[46] WorldPop, "Global 1km Population total adjusted to match the corresponding UNPD estimate." University of Southampton, Jun. 22, 2020. doi: 10.5258/SOTON/WP00671.
[47] P. Gauthier, A. Furno, and N.-E. El Faouzi, "Road Network Resilience: How to Identify Critical Links Subject to Day-to-Day Disruptions," *Transportation Research Record*, vol. 2672, no. 1, pp. 54–65, Dec. 2018, doi: 10.1177/0361198118792115.
[48] H. Chmielewski, R. Guidotti, T. McAllister, and P. Gardoni, "Response of Water Systems under Extreme Events: A Comprehensive Approach to Modeling Water System Resilience," pp. 475–486, May 2016, doi: 10.1061/9780784479865.050.
[49] M. Ouyang, L. Hong, Z.-J. Mao, M.-H. Yu, and F. Qi, "A methodological approach to analyze vulnerability of interdependent infrastructures," *Simulation Modelling Practice and Theory*, vol. 17, no. 5, pp. 817–828, May 2009, doi: 10.1016/j.simpat.2009.02.001.
[50] D. N. Bresch and G. Aznar-Siguan, "CLIMADA v1.4.1: towards a globally consistent adaptation options appraisal tool," *Geoscientific Model Development*, vol. 14, no. 1, pp. 351–363, Jan. 2021, doi: 10.5194/gmd-14-351-2021.
[51] S. Eberenz, D. Stocker, T. Röösli, and D. N. Bresch, "Asset exposure data for global physical risk assessment," *Earth System Science Data*, vol. 12, no. 2, pp. 817–833, Apr. 2020, doi: https://doi.org/10.5194/essd-12-817-2020.
[52] P. M. Kam *et al.*, "Global warming and population change both heighten future risk of human displacement due to river floods," *Environ. Res. Lett.*, vol. 16, no. 4, p. 044026, Mar. 2021, doi: 10.1088/1748-9326/abd26c.
[53] I. J. Sauer *et al.*, "Climate signals in river flood damages emerge under sound regional disaggregation," *Nature Communications*, vol. 12, no. 1, Art. no. 1, Apr. 2021, doi: 10.1038/s41467-021-22153-9.
[54] M. Souvignet, F. Wieneke, L. Mueller, and D. N. Bresch, "Economics of Climate Adaptation (ECA) - Guidebook for Practitioners," 2016.
[55] N. Bloemendaal, H. de Moel, J. M. Mol, P. R. M. Bosma, A. N. Polen, and J. M. Collins, "Adequately reflecting the severity of tropical cyclones using the new Tropical Cyclone Severity Scale," *Environ. Res. Lett.*, vol. 16, no. 1, p. 014048, Jan. 2021, doi: 10.1088/1748-9326/abd131.
[56] G. Holland, "A Revised Hurricane Pressure–Wind Model," *Mon. Wea. Rev.*, vol. 136, no. 9, pp. 3432–3445, Sep. 2008, doi: 10.1175/2008MWR2395.1.

[57] R. Fausset, A. Blinder, and M. Haag, “Rescue Teams Scour Ruins as Hurricane Death Toll Rises,” *The New York Times*, Oct. 12, 2018. Accessed: Feb. 14, 2022. [Online]. Available: https://www.nytimes.com/2018/10/12/us/hurricane-michael-live-updates-florida.html
[58] E. Jenelius and L.-G. Mattsson, “Road network vulnerability analysis of area-covering disruptions: A grid-based approach with case study,” *Transportation Research Part A: Policy and Practice*, vol. 46, no. 5, pp. 746–760, Jun. 2012, doi: 10.1016/j.tra.2012.02.003.
[59] K. M. de Bruijn, L. Cumiskey, R. N. Dhubhda, M. Hounjet, and W. Hynes, “Flood vulnerability of critical infrastructure in Cork, Ireland,” *E3S Web Conf.*, vol. 7, p. 07005, 2016, doi: 10.1051/e3sconf/20160707005.
[60] P. Gauthier, A. Furno, and N.-E. El Faouzi, “Road Network Resilience: How to Identify Critical Links Subject to Day-to-Day Disruptions,” *Transportation Research Record*, vol. 2672, no. 1, pp. 54–65, Dec. 2018, doi: 10.1177/0361198118792115.
[61] C. R. Zorn and A. Y. Shamseldin, “Quantifying Directional Dependencies from Infrastructure Restoration Data,” *Earthquake Spectra*, vol. 32, no. 3, pp. 1363–1381, Aug. 2016, doi: 10.1193/013015EQS015M.
[62] C. Zorn, R. Pant, S. Thacker, and A. Y. Shamseldin, “Evaluating the Magnitude and Spatial Extent of Disruptions Across Interdependent National Infrastructure Networks,” *ASME J. Risk Uncertainty Part B*, vol. 6, no. 2, Jun. 2020, doi: 10.1115/1.4046327.
[63] E. Luiijf, A. Nieuwenhuijs, M. Klaver, M. van Eeten, and E. Cruz, “Empirical Findings on Critical Infrastructure Dependencies in Europe,” in *Critical Information Infrastructure Security*, Berlin, Heidelberg, 2009, pp. 302–310. doi: 10.1007/978-3-642-03552-4_28.
[64] K. Poljansek, M. Marín Ferrer, T. De Groeve, and I. Clark, “Science for disaster risk management 2017: knowing better and losing less,” ETH Zurich, Report, 2017. Accessed: Jun. 08, 2020. [Online]. Available: https://www.research-collection.ethz.ch/handle/20.500.11850/297819
[65] A. Naqvi and I. Monasterolo, “Natural Disasters, Cascading Losses, and Economic Complexity: A Multi-layer Behavioral Network Approach,” Apr. 2019. https://epub.wu.ac.at/6914/ (accessed Apr. 28, 2022).
[66] A. Otsuka, “Natural disasters and electricity consumption behavior: a case study of the 2011 Great East Japan Earthquake,” *Asia-Pac J Reg Sci*, vol. 3, no. 3, pp. 887–910, Oct. 2019, doi: 10.1007/s41685-019-00129-4.
[67] M. Ghosn *et al.*, “Performance Indicators for Structural Systems and Infrastructure Networks,” *Journal of Structural Engineering*, vol. 142, no. 9, p. F4016003, Sep. 2016, doi: 10.1061/(ASCE)ST.1943-541X.0001542.
[68] D. Henry and J. Emmanuel Ramirez-Marquez, “Generic metrics and quantitative approaches for system resilience as a function of time,” *Reliability Engineering & System Safety*, vol. 99, pp. 114–122, Mar. 2012, doi: 10.1016/j.ress.2011.09.002.
[69] Y. Almoghathawi, K. Barker, and L. A. Albert, “Resilience-driven restoration model for interdependent infrastructure networks,” *Reliability Engineering & System Safety*, vol. 185, pp. 12–23, May 2019, doi: 10.1016/j.ress.2018.12.006.
[70] L. I. E. E., J. E. Mitchell, and W. A. Wallace, “Restoration of Services in Interdependent Infrastructure Systems: A Network Flows Approach,” *IEEE Transactions on Systems, Man, and Cybernetics, Part C (Applications and Reviews)*, vol. 37, no. 6, pp. 1303–1317, Nov. 2007, doi: 10.1109/TSMCC.2007.905859.
[71] S. Hasan and G. Foliente, “Modeling infrastructure system interdependencies and socioeconomic impacts of failure in extreme events: emerging R&D challenges,” *Nat Hazards*, vol. 78, no. 3, pp. 2143–2168, Sep. 2015, doi: 10.1007/s11069-015-1814-7.
[72] D. Mitsova, A. Sapat, A.-M. Esnard, and A. J. Lamadrid, “Evaluating the Impact of Infrastructure Interdependencies on the Emergency Services Sector and Critical Support Functions Using an Expert Opinion Survey,” *Journal of Infrastructure Systems*, vol. 26, no. 2, p. 04020015, Jun. 2020, doi: 10.1061/(ASCE)IS.1943-555X.0000548.
[73] S. L. Cutter, B. J. Boruff, and W. L. Shirley, “Social Vulnerability to Environmental Hazards,” in *Hazards Vulnerability and Environmental Justice*, Routledge, 2006.
[74] De Leonardis, D., Huey, R., and Green, J., “National Traffic Speeds Survey III: 2015,” National Highway Traffic Safety Administration, Washington, DC, DOT HS 812 485, Mar. 2018.
[75] J. Guo, T. Feng, Z. Cai, X. Lian, and W. Tang, “Vulnerability Assessment for Power Transmission Lines under Typhoon Weather Based on a Cascading Failure State Transition Diagram,” *Energies*, vol. 13, no. 14, 2020, doi: http://dx.doi.org/10.3390/en13143681.
[76] “Hazus Hurricane Model Technical Manual,” FEMA, Mar. 2021. Accessed: Mar. 10, 2022. [Online]. Available: https://www.fema.gov/sites/default/files/documents/fema_hazus-hurricane-technical-manual-4.2.3_0.pdf
[77] G. Holland, “A Revised Hurricane Pressure–Wind Model,” *Mon. Wea. Rev.*, vol. 136, no. 9, pp. 3432–3445, Sep. 2008, doi: 10.1175/2008MWR2395.1.

Annex

A. Formal treatment of the developed modelling chain

G^j	graph of CI network j
n_i^j	i[th] node in G^j
e_{mn}^j	directed edge from n_m^j to n_n^j
G	interdependent CI graph, spanning all graphs $G^j, G^k, \ldots$ of investigated CI networks and all e^{jk}
e_{mn}^{jk}	directed dependency edge from n_m^j to n_n^k
G'^j	subgraph of G spanning all elements of G^j
G'^{jk}	subgraph of G, spanning all elements G^j, G^k and e^{jk}
A^{jk}	adjacency matrix of G'^{jk}
L_i	geo-spatial location of graph element i (node and edge attribute)
F_i	functional state of graph element i (node and edge attribute)
I_i	structural damage ('impact') of graph element i (node and edge attribute)
E_i	exposure value of graph element i (node and edge attribute)
D_i	damage threshold of graph element i (node and edge attribute)
C_i^{jk}	capacity for node i for type of flow passing between CI types j and k (node attribute)
T_i^{jk}	capacity threshold for node i for type of flow passing between CI types j and k (node attribute)
M_i^{jk}	capacity supply at node i for type of flow passing between CI types j and k (node attribute)
S_i^j	service supply at node i for type of flow delivered by CI type j (node attribute)
$H(L)$	hazard intensity at L
$V(H)$	hazard intensity-dependent vulnerability curve

Initialization

0. $\forall\ j$ create G^j with n^j(nodes-only) or n^j, e^j (nodes and edges) and set attributes $L,\ F,\ D,\ E,\ X$
   L: geo-location in latitude and longitude; specific to each n_i^j, e_i^j
   F: functional state ({0, 1}). Set to 1 $\forall\ n^j, e^j \in G^j$
   D: fraction (]0, 1]) of structural damage I beyond which $F \to 0$; specific to n^j, e^j
   E: value of the physical network element - set to 1 $\forall\ n^j, e^j \in G^j$
   X: further attributes specific to n^j and/or e^j
1. Create interdependent CI graph $G = \sum_j G^j$
   $\forall$ combinations of (jk) in list of identified CI dependencies:
   Create e_{mn}^{jk} between n_m^j and n_n^k if linking conditions (distance, redundancy criterion, etc.) fulfilled
   Assign node attributes $C^{jk}, T^{jk}\ \forall\ n \in G$:
   $$C_i^{jk}: \begin{cases} -1 \text{ if } n_i^j \\ 1 \text{ if } n_i^k \\ 0 \text{ else} \end{cases}, \quad T_i^{jk}: \begin{cases} [0,1]\ n_i^k \\ 0 \text{ else} \end{cases}$$

Flow Assignment & Functional State Update

2. $\forall\ j$ where $G^j \ni\ n^j, e^j$: extract G'^j from G.
   Perform internal flow calculations according to adequate algorithm.
   Update $C^{jk},\ F\ \forall n^j$ in G, where required.
3. $\forall$ combinations of (jk) where $k \neq 'people'$, extract G'^{jk} from G; update $F\ \forall\ n^k$:
   $M^{jk} = \left(F \cdot C^{jk}\right)^T * A^{jk};\ F = \min\left(F,\ M^{jk} \geq T^{jk}\right)$
4. Repeat 2. and 3. until $\Delta F = 0$

Basic Service Access Determination

5. $\forall$ combinations of $(j, people)$, extract $G'^{j,people}$ from G. Assign attribute S^j to n^{people}:
   $M^{j,people} = \left(F \cdot C^{j,people}\right)^T * A^{j,people}$
   $S^j = \left(M^{j,people}\ \geq T^{j,people}\right)$

Natural Hazard Impact Calculation & Functionality State Update

6. Assign structural damage attribute $I\ \forall\ n, e \in G$:
   $I = H(L) * V(H) * E$
7. Update $F\ \forall\ n, e \in G$:
   $F = \min\left(F, I \leq D\right)$

Cascade & Functional State Updates

8. Update $C^{jk},\ F\ \forall\ n, e\ \forall (jk, k \neq people)$ in G according to 2. - 4.

Basic Service Access Update

9. If road access is a linking condition for dependency combination $(j, people)$:

Re-check path existence and length of path between $n^j, n^{people}\ \forall\ e^{j,people}$; else delete $e^{j,people}$ from G

10. Update $S^j\ \forall\ n^{people}$, $\forall\ (j, people)$; see step 5.

B. Modelling Choices for CI Networks

B.1. Network Components

Table B.1 CI networks and their components, in edges (E) and nodes (N). First column suggests the minimally needed component data to represent the system in a standardized low-complexity setting, second column proposes additional components if data is at hand.

CI system	Simplified representation	Extension possibilities
Road	N: intersections E: streets	N: tunnels, bridges E: -
Electric Power	N: power generation plants E: transmission lines	N: transmission & distribution substations, power poles E: low-voltage distribution lines
Telecommunication	N: cell towers E: -	N: internet exchange points, data centres, central offices, base stations, poles E: landlines, fibre-optic cables, submarine transmission lines
Wastewater & Water Supply	N: water treatment plants E: -	N: wells, reservoirs, tanks, cisterns, pumps, water bodies E: water pipelines, water tunnels, rivers
Healthcare & Emergency Services	N: hospitals, clinics E: -	N: doctors' practices, dentists, pharmacies, nursing homes
Educational Facilities	N: schools E:	N: universities, childcare centres, kindergartens
End-users	N: people clusters E: -	

B.2. Network Dependencies

For a detailed list of CI dependencies based on literature review, see Supplementary Materials.

C. Case Study

C.1. Input Data

Infrastructure Data

*Table C.1 Geo-coded infrastructure asset data used in the case study, chapter 3. *) HIFLD: Homeland Infrastructure Foundation-Level Data*

Infrastructure	Source	Data description, Pre-processing
Roads	OpenStreetMap	*Data*: Retrieved from data dump at geofabrik.de for states FL, AL, GA matching tags highway= (motorway | motorway_link | trunk | trunk_link | primary| primary_link) using the openstreetmap module in CLIMADA. *Pre-processing*: Line merging, roundabout cleaning, duplicate removal, linking unconnected cluster
Hospitals	HIFLD*: Hospitals	*Data:* All amenities in states FL, AL, GA incl. 20kms buffer around outer borders *Pre-processing*: -
Power lines	HIFLD: Electric Power Transmission Lines	*Data:* All lines in in states FL, AL, G *Pre-processing*: Line merging, duplicate removal, linking unconnected cluster
Power plants	HIFLD: Power Plants	*Data:* All amenities in states FL, AL, GA incl. 20 km buffer around outer borders *Pre-processing*: -
Educational Facilities	HIFLD: Public Schools	*Data:* All amenities in states FL, AL, GA incl. 20 km buffer around outer borders *Pre-processing*: -
Cell Towers	HIFLD: Cellular Towers	*Data:* All amenities in states FL, AL, GA incl. 20 km buffer around outer borders *Pre-processing*: -

Wastewater	HIFLD: Wastewater Treatment Plants	*Data:* All amenities in states FL, AL, GA incl. 20 km buffer around outer borders *Pre-processing*: -
People	WorldPop Gridded Population Count	*Data:* United States of America, 1km UN-adjusted, 2020. *Pre-processing*: Re-gridded raster data on population counts to resolution of 10 km x10 km, vectorized, cropped at outer borders of states FL, AL, GA

Power Supply & Demand Data

Table C.2 Population data, energy supply and demand data used for case study in Chapter 3.

Variable	Source	Data description
Supply	HIFLD: Power Plants	Same data source as for geo-location data of power plants in the region of interest. Electric energy supply taken from power plants net annual generation, given in column *NET_GEN.*
Demand	International Energy Agency (IEA) World Energy Balances	Total electric energy consumption for entire USA, all sectors, 2019.

Calculation of electric power demand per people cluster (cf. Table C.1): Total electric energy consumption / total US-population * population count of cluster

Calculation of electric power supply per power plant (cf. Table C.1): Directly taken from data source.

Supply / demand balancing in undisrupted state: Addition of an import/export element to the power plant data frame with supply amounting to difference between total power plants supply in region of interest and total energy consumption in region of interest.

Dependencies

Table C.3 Dependencies identified between CI networks (#1-#10) and between CI networks and end-users (#11-#16). Dependency parametrizations are used to link individual CI graphs and population graph into one interdependent CI graph. Decisions for certain parameter settings are discussed in the paragraph below.

Dep	source	target	Redun-dancy	Road access	Dep. type	Flow type	Func. Thresh	Dist. Thresh. [m]
1	power line	celltower	FALSE	FALSE	functional	physical	0.6	-
2	celltower	education	TRUE	FALSE	functional	logical	1	40’000
3	power line	education	FALSE	FALSE	functional	physical	0.6	-
4	wastewater	education	FALSE	FALSE	functional	logical	1	-
5	celltower	health	TRUE	FALSE	functional	logical	1	40’000
6	power line	health	FALSE	FALSE	functional	physical	0.6	-
7	wastewater	health	FALSE	FALSE	functional	logical	1	-
8	celltower	power plant	TRUE	FALSE	functional	logical	1	40’000
9	celltower	wastewater	TRUE	FALSE	functional	logical	1	40’000
10	power line	wastewater	FALSE	FALSE	functional	physical	0.6	-
11	celltower	people	TRUE	FALSE	enduser	logical	1	40’000
12	education	people	FALSE	TRUE	enduser	logical	1	40’000
13	health	people	FALSE	TRUE	enduser	logical	1	100’000
14	power line	people	FALSE	FALSE	enduser	physical	0.6	-
15	road	people	TRUE	FALSE	enduser	logical	1	30’000
16	wastewater	people	FALSE	FALSE	enduser	logical	1	-

Selection of distance thresholds: A combination of sophisticated guess (such as 40 km being a generous diameter of a cell site around a cell tower or hospitals being at most 100 km from persons, which equals a travel time of little more than the “golden hour” crucial in medical emergencies, when considering average travel speeds on a highway [74]), and iterative

refinements such that service access levels in stage IV were >99% for all basic services across the area of investigation in a base state simulation with undamaged CIs. For dependencies where no distance thresholds are set, target elements are linked to the closest element of the respective source type, irrespective of its distance. This is the case for all non-redundant dependencies where it is obvious that such a link must exist (e.g. educational and healthcare facilities having power and water access).

Selection of redundancy specification: Dependencies which feature a physical commodity flow from source to target (here, water and power) are hypothesized to have one non-redundant physical connection from source to target. Mobile communication is modelled to be provided from any source within distance thresholds, as connectivity can be established through any reachable cell site. Healthcare can be provided from any reachable healthcare facility, but school enrolments are usually fixed, hence each population clusters dispose of only one non-substitutable education link. Road access is assumed to be provided by any reachable road within distance threshold.

Selection of flow types and functionality thresholds: Physical metrics for demand and supply were readily available for the power system, hence power dependencies could be parametrized by a physically informed 'capacity' at which power is provided (given as the ratio of power demand to power supply in each network cluster). Functionality thresholds for power dependencies can therefore be expressed as fraction of the regular power supply which is still tolerated before a dependent component turns dysfunctional. It was set here to 0.6 in absence of any component-specific information, to interpreted as "if demand-to-supply ratio in the power network cluster to which the dependent component is linked, drops below 0.6, the component will turn dysfunctional". All other dependencies are, in absence of physically informed flow metrics, logical dependencies. As such, they either provide supply from a functional source, or they do not, if the source is dysfunctional. Functionality thresholds for logical dependencies are hence trivial and set to 1.

Interdependent CI graph characteristics

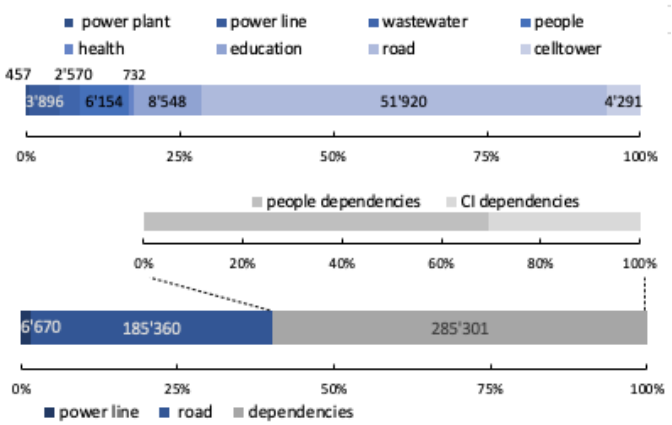

Figure C.1 Specifications of node (1st bar plot) and edge elements (2nd bar plot) in the interdependent CI graph, constructed for the case presented in section 3.1.

Hazard & Vulnerability

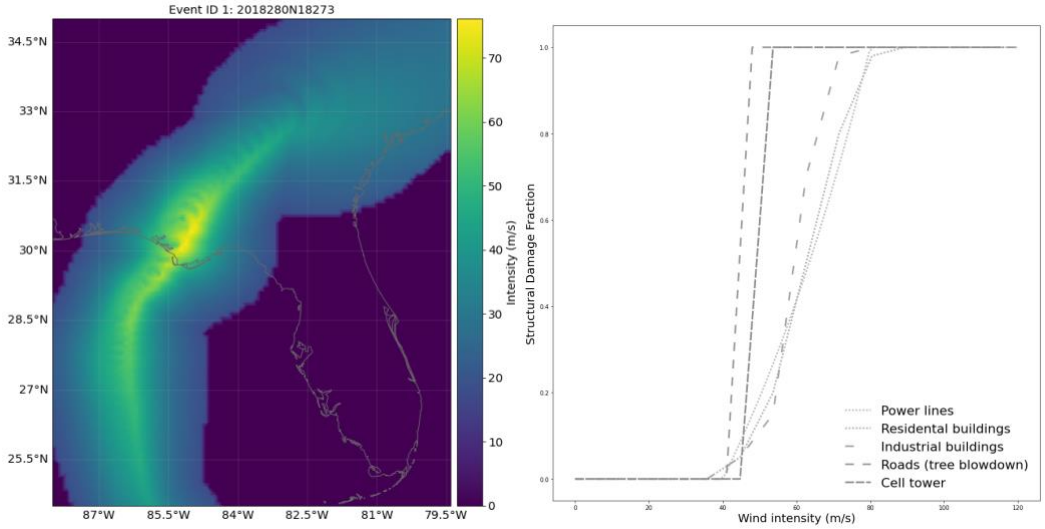

Figure C.2 Map of Hurricane Michael wind-field intensity, computed with CLIMADA from Michael's hurricane track. Track data from IBTrACS, implemented wind field algorithm from [77].

Figure C.3 Impact functions used for structural damage calculations from hurricane wind field in section 3.1, for all CI types. Note that y-axis represents fraction of structural damage to components for all CIs except power lines, for which it is failure probability. Sources: power lines in [58], residential building and industrial building (both for z=0.35) in [76], roads in [9], cell towers: step function taken from interview with cell tower provider stating they are "built to withstand winds of up to 110 miles per hour".

C.2. Sensitivity Analysis

Table C.4 Scenarios to study the sensitivity of end results (number of people experiencing basic service disruptions) to assumptions throughout the modelling chain. For parameterizations details, see section C.2.

Scenario	Description	Stage
No CI inter-dependencies	Removing any dependencies between CI types.	I
Dependency parametrization	Decreasing distance thresholds for end-user dependencies.	I / IV
Dependency parametrization	Increasing distance thresholds for end-user dependencies.	I / IV
High component vulnerability	Shifting impact functions towards lower hazard intensities.	II
Low component vulnerability	Shifting impact functions towards higher hazard intensities	II
High functionality threshold	Increasing damage thresholds for component dysfunctionality	II
Low functionality threshold	Decreasing damage thresholds for component dysfunctionality	II

Table C.5 Results of sensitivity analysis: Amount of people experiencing service disruptions in each scenario due to hazard-induced failure cascades, relative to disruption numbers in base scenario. Selected scenarios as described in chapter 3.2: altering impact functions (columns high / low vulnerability), shifting damage thresholds for component dysfunctionality (columns low / high damage threshold), leaving out interdependencies (column no CI interdependencies), modifying dependency establishment conditions (columns lower / higher distance threshold). 'Base scenario' refers to case study as described in chapter 3.1. Parametrizations of those scenarios are listed in the paragraphs below.

Access to Basic Service	High vuln.	Low vuln.	Low dmg. threshold	High dmg. threshold	No CI interdeps	Lower dist. thresh.	Higher dist. thresh
Mobility	247%	0%	109%	96%	100%	101%	100%
Power	202%	32%	102%	97%	47%	151%	0%
Healthcare	261%	0%	100%	100%	16%	468%	0%
Education	191%	27%	102%	96%	40%	338%	0%

Mobile Comms.	247%	14%	101%	97%	50%	118%	12%
Water Supply	213%	0%	100%	100%	41%	259%	0%

Scenarios 'High & Low Vulnerability': Impact Functions

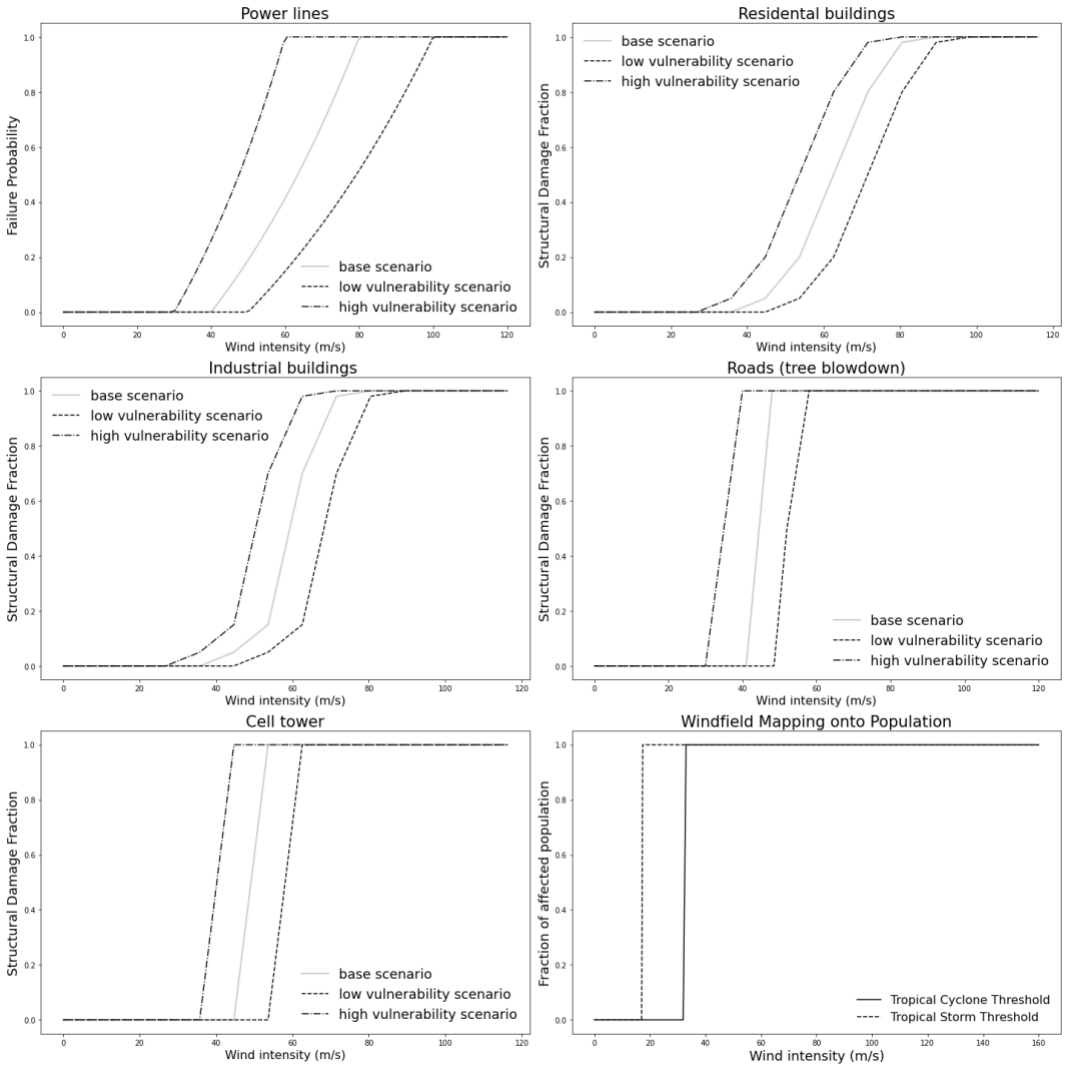

Figure C.4 Impact functions used for base case (gray, solid), low vulnerability scenario (black, dotted) and high vulnerability scenario (black, dashed). x-axes: hurricane wind strength (m/s), y-axes: failure probability (power lines), structural damage fraction (all other CIs).

Scenarios 'Damage-Functionality Thresholds'

Table C.6 Threshold of structural component damage (averaged over length of section for edge-type CIs such as powerlines & roads), which leads to an assignment of internal functional level of 0.

Scenario	**Base**	**Low**	**High**
Threshold	0.3	0.15	0.5

Scenario 'No CI interdependencies'

Table C.7 Dependency conditions used in the scenario w/o inter-CI links.

Dep	**source**	**target**	**Redun-dancy**	**Road access**	**Dep. type**	**Flow type**	**Func. Thresh**	**Dist. Thresh. [m]**
11	cell tower	people	TRUE	FALSE	end user	logical	1	40000

12	education	people	FALSE	TRUE	end user	logical	1	40000
13	health	people	TRUE	TRUE	end user	logical	1	100000
14	power line	people	FALSE	FALSE	end user	physical	0.6	
15	road	people	TRUE	FALSE	end user	logical	0.5	30000
16	wastewater	people	FALSE	FALSE	end user	logical	0.1	

Scenario 'Lower & higher distance thresholds

Table C.8 Dependency conditions for scenario with modified parametrizations compared to base case (lower and higher distance thresholds).

Dep	Source	Target	Redun-dancy	Road access	Dep. type	Flow type	Func. Thresh	Dist. Thresh. [m]
1	power line	cell tower	FALSE	FALSE	functional	physical	0.6	
2	cell tower	education	TRUE	FALSE	functional	logical	1	40000
3	power line	education	FALSE	FALSE	functional	physical	0.6	
4	wastewater	education	FALSE	FALSE	functional	logical	1	
5	cell tower	health	TRUE	FALSE	functional	logical	1	40000
6	power line	health	FALSE	FALSE	functional	physical	0.6	
7	wastewater	health	FALSE	FALSE	functional	logical	1	
8	cell tower	power plant	TRUE	FALSE	functional	logical	1	40000
9	cell tower	wastewater	TRUE	FALSE	functional	logical	1	40000
10	power line	wastewater	FALSE	FALSE	functional	physical	0.6	
11	cell tower	people	TRUE	FALSE	end user	logical	1	40000
12	education	people	FALSE	TRUE	end user	logical	1	40'000 / 25'000
13	health	people	TRUE	TRUE	end user	logical	1	130'000 / 70'000
14	power line	people	FALSE	FALSE	end user	physical	0.6	
15	road	people	TRUE	FALSE	end user	logical	1	40'000 / 20'000
16	wastewater	people	FALSE	FALSE	end user	logical	1	

C.3. Validation Sources

See Supplementary Material.